A Chemical Biology Platform to Develop Small Molecule Probes for Bromodomains

A dissertation presented

by

Katharin L. Shaw

to

The Committee on Higher Degrees in Chemical Biology

in partial fulfillment of the requirements

for the degree of

Doctor of Philosophy

in the subject of

Chemical Biology

Harvard University

Cambridge, Massachusetts

February 2017

Dissertation Advisor: Professor James E. Bradner **Katharin Shaw**

A Chemical Biology Platform to Develop Small Molecule Probes for Bromodomains

Abstract

Bromodomain epigenetic reader proteins play crucial roles in the pathogenesis of diseases ranging from inflammation to cancer. Small molecule inihibitors have engendered a nuanced understanding of the role of BET subfamily bromodomains in multiple diseases. Here, platforms were established to facilitate chemical probe development for the remaining ~50 bromodomains with a concentrated focus on establishing a pipeline for the discovery of CBP bromodomain inhibitors.

CBP is a large bromodomain-containing transcriptional co-activator involved in cell proliferation and growth, cellular differentiation and development, cognitive function, and cell adhesion. It is involved in the pathogenesis of cancer, in particular hematologic diseases. A high-throughput biochemical assay, cellular viability assay, and cellular target engagement assay were established in order to screen and validate small molecule inhibitors of the CBP bromodomain. A family-wide bromodomain profiling platform (BROMO*scan*) was established and fully validated to provide broad quantitative binding affinity and selectivity information. Using this platform, novel small molecule inhibitors for non-BET domains were discovered. Moreover, a LRRK2 kinase inhibitor with potent bromodomain cross-reactivity was identified and optimized. Using

BROMO*scan* and the CBP bromodomain assays deeloped here, a dually functioning kinase-bromodomain inhibitor was discovered that was potent and selective for CBP.

Table of Contents

Acknowledgments

“Like art, I suspect you know chemical biology when you see it.” — Jay Bradner

Being in Jay’s lab has afforded me the unique opportunity to participate in disciplines as diverse as organic chemistry, biochemistry, molecular and cell biology, and computational biology. By now, I suspect I know chemical biology when I see it.

When I first joined the Bradner lab, Jay asked me what I most wanted to learn over the course of graduate school and what I needed from him to accomplish my goals. Having had no clear idea at the time, I told him, “Everything.” He laughed at me, but he proceeded to provide an environment so rich I was limited only by own time and capacity. By far the most valuable resources Jay provided are people— peers and mentors who are remarkable for their character as much as their talent. I am grateful and humbled to work with and alongside all of them.

Jun Qi has been my mentor and my friend throughout every step of my graduate career. He is a wellspring of invaluable advice, scientific and personal. He is responsible for teaching me the practice of organic chemistry and for keeping me from making stupid mistakes. I collaborated closely with him on nearly every one of my projects. Chris Ott and Rhamy Zeid have been invaluable examples of rigorous scientists. I am thankful for the countless hours Chris spent teaching me how to think through biological problems. He is exacting in both design and execution, and I am confident to have learned from the best. Rhamy walked me through my first time in nearly every molecular biology technique I learned. His time, patience, and understanding comprise the cornerstone of my biological expertise. Much of the work I did in the last half of my PhD

was in collaboration with Dennis Buckley. He has been my sounding board about everything from chemistry to project direction to career planning to the construction of a perfectly balanced cocktail. When he joined the lab, I found not only a scientific partner but also one of my closest friends.

I am incredibly grateful for Michael McKeown— my classmate, my labmate, my benchmate, my wedding planner, and my groomsman. For approximately five years, I spent almost all of my waking hours with him. When I was stuck in an experimental mire, Michael was always ready to offer me a helping hand (or whiskey, if my failure seemed certain). I would not be the scientist, or even person, that I am today without him. Ron Paranal, who is one of the most published members of the Bradner lab, felt that his CV would be incomplete without a dissertation. I acknowledge that Ronald owns a ten percent emotional stake in my PhD for all of the love, support, and validation that he's offered over the years.

In addition to lab members, my program coordinators and my dissertation advisory committee were instrumental in shaping my time here. Samantha Reed, KeyAnna Schmiedl, and Jason Millberg have worked tirelessly to ensure that my education here goes smoothly. I am so very grateful to Professors Stephen Blacklow, Nathanael Gray, and Jon Clardy for the time and care that they have invested in me. I look up to each of them as the kind of rigorous, insightful scientist I want to be. Their mentorship has been invaluable.

My experience as a graduate student begins and ends with Jay. His influence on my scientific development is evident in every poster, every talk, every grant, every

paper I have produced in graduate school. Jay has taught me to be absurdly, alarmingly bold; to reach always beyond my grasp; to keep heart when I fail and nerve when I succeed; and to stand behind my convictions with all of the force of my personality. But of the myriad things I have learned from Jay, perhaps the most important was how to craft a story with assiduity and panache. Scientific knowledge is a collection of stories—the stories we observe and the stories we tell each other.

The story that I am presenting here started, in many ways, long before I ever arrived at Harvard. I doubt I will ever have the skill to adequately convey my gratitude for everything my family has given and sacrificed so that I could be where I am now. To my grandparents, to Mommy and Daddy and my sister— I love you.

I am indebted to all of the following educators. They invested more into me than I deserved, and were it not for their super-human feats of patience and their willingness to teach me to direct my energy, I would not be where I am now. My Scottish Highland dance teacher Eleanor Unger taught me that success is earned with commitment, persistence, and discipline. When I make a mistake, when I am exhausted, when I think I've reached the limits of my patience and effort, it is still her voice I hear saying, "Again!" I was fortunate to have exceptional high school science teachers. Clare Kerr and Camilla Walck fostered my interest in chemistry and biology, providing me with opportunities to further my scientific education far above and beyond their responsibilities as teachers. My academic advisors, Professors Gerald Seebach and Eva Csuhai, taught many of my chemistry courses and introduced me to scientific research. They are, in large part, a reason I chose to go to graduate school. I owe Dr. Ulrike Eggert a great deal for her time and mentorship during my summer

undergraduate research experience and throughout the graduate school application process. She introduced me to the field of Chemical Biology, where I first encountered research that applied chemical tools and principles to the study of biological mechanisms with mindful, rigorous intent.

I am also thankful to all of the people I am fortunate to call my friends. They have given me so much of their time and love and support, and I know nothing that I accomplish is done in isolation. To Rachel, Ketron, Anthony, and Jaime, I owe you any service you require. Keep the $5. First and foremost among them is my best friend and husband— Andrew Alexander. He has been by my side for over a decade through countless (mis)adventures. He is kind and understanding, and he has put up with me complaining about nearly everyone I've thanked here. Last and actually least, I'd like to thank George Eliot and Charles Dickens, for providing me with inspiration and amusement after each long day. Sadly, neither of them will ever realize nor care how much they've enriched my life— because they're inconsiderate little beasts, as cats are wont to be.

Chapter 1

Bromodomain Function in Gene Regulation and Cancer

Epigenetics and Cancer

Epigenetic information, comprising the heritable changes in gene expression caused by mechanisms other than alterations to DNA sequence, is transmitted through cell division via covalent modifications to DNA or histone proteins. These post-translational modifications include DNA methylation and histone methylation, acetylation, phosphorylation, sumoylation, ubiquitination, and others. Epigenetic modifications are responsible for cellular “memory,” serving as molecular bookmarks for maintaining specific patterns of gene expression through mitotic progression. Depending on the modification, genes may be profiled for reactivation or for permanent silencing upon cell division. Apart from inheritence, epigenetic modifications and their respective chromatin modifying enzymes also maintain a dynamic chromatin state that influences chromatin compaction and transcriptional regulation. In eukaryotes, large genomic size requires the compaction of genetic material not involved in transcription. This compaction is effected through the regulation of chromatin structure and the mediation of transcriptional complex assembly via the wrapping of DNA around histones and subsequent higher-order folding. Histones are highly conserved protein complexes comprised of two H2A-H2B dimers and a H3-H4 tetramer. The unstructured tail regions of histones are heavily modified by nuclear enzymes; these modifications affect higher-order chromatin structure and mediate transcriptional complex assembly, regulating gene expression (Figure 1.1) (*1*-*3*).

The modification of histones is highly dynamic, with specialized enzymes catalyzing their introduction (‘writers’) or removal (‘erasers’). Examples include histone acetyltransferases (HATs), histone deacetylases (HDACs), histone methyltransferases

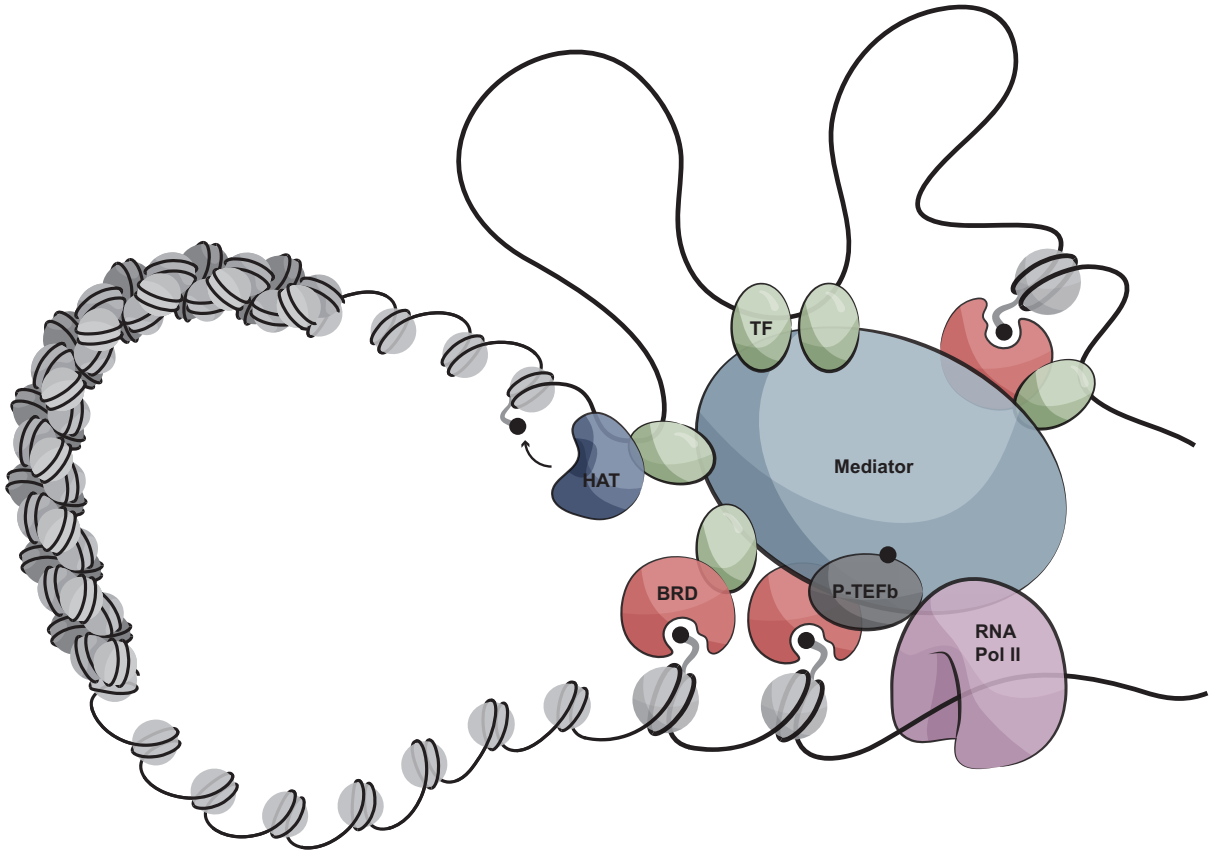

Figure 1.1 Chromatin Modifying Proteins and Transcription Chromatin modifications maintain a dynamic chromatin state, influencing chromatin compaction and thus the assembly of transcriptional machinery. Chromatin modifying enzymes and reader proteins associate with transcription factors and the basal transcription machinery to regulate gene expression.

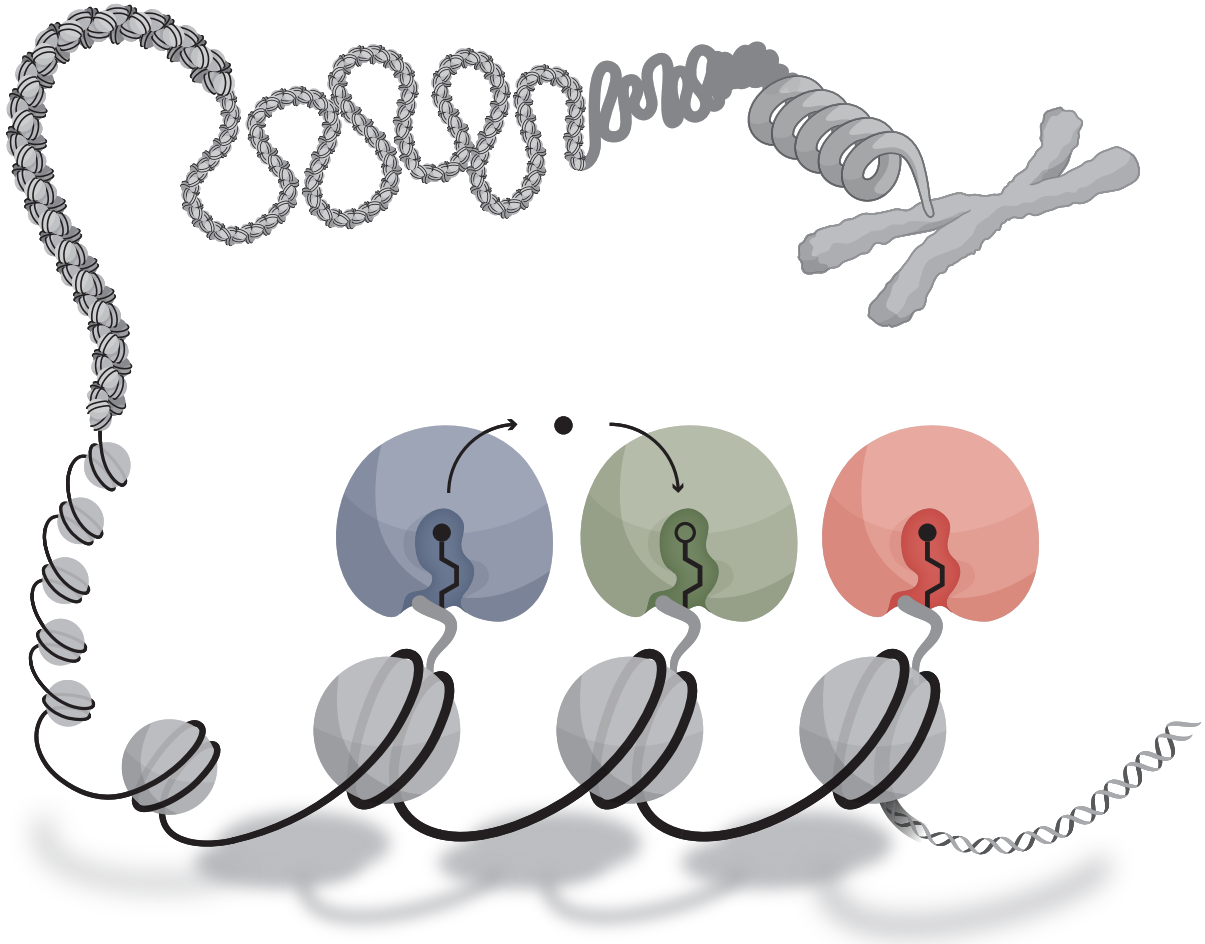

Figure 1.2 Chromatin Erasers, Writers, and Readers Histone modification is a dynamic process, in which “erasers” and “writers” remove and introduce particular marks. Chromatin binding modules, or chromatin readers, recognize posttranslational marks.

(HMTs) and histone demethylases. These enzyme systems are found as part of multi-protein complexes involved in transcriptional regulation, DNA replication and DNA repair. Likewise, chromatin binding modules or epigenetic “readers” are also incorporated into these large multi-unit complexes. Readers are often regarded as functional “effector” proteins that can recognize particular post-translational modifications (e.g. methylation or acetylation marks) on histone proteins or DNA (Figure 1.2).

The dysregulation of epigenetic modifying enzymes and the resulting inappropriate changes to chromatin modifications lead to the disruption of the chromatin signaling network, resulting in aberrent gene expression and silencing. In cancer, epigenetic proteins are among the most promising and intently pursued targets in drug discovery (*4*). This relates to the growing appreciation that deregulation of gene regulatory pathways via chromatin complex alterations is a hallmark feature of cancer. Chromatin-associated complexes have recently been identified as recurrently altered or transcriptionally deregulated in many cancers, including but not limited to, TET methylcytosine dioxygenase 2 (TET2), DNA methyltransferase 3A (DNMT3A), enhancer of zeste homologue 2 (EZH2) in lung cancer (*5*), the histone lysine methyltransferase MMSET in multiple myeloma (*6*), bromodomain BRD4 in NUT midline carcinoma (*7, 8*), and acetyl-transferase and bromodomain CBP in acute myeloid leukemia (*9*). Notably, each of these factors influences chromatin structure, and has been linked to coordinated regulation of normal developmental transcriptional pathways (*10-13*). These data establish the hypothesis that disruption of chromatin architecture is a common event in cancer pathogenesis, either permissive with or distinct from oncogenic

signaling pathways, functioning to deregulate transcriptional programs associated with cellular differentiation.

Among all targets in chromatin biology, histone deacetylases (HDACs) have commanded significant attention due to their control of cancer gene regulatory pathways involved in proliferation and survival, and owing to the broad anti-neoplastic effect of direct-acting inhibitors in models of cancer (*14*). HDAC inhibition has been linked to numerous potential and beneficial therapeutic uses, broadly in cancer and also in inflammation and neurodegenerative diseases. To date, four HDAC inhibitors, Vorinostat, Romidepsin, Panobinostat, and Belinostat, have successfully proceeded through clinical testing and are approved for the tratment of hematologic cancers. Clinical trials are continuously expanding to address other types of cancer and also nonmalignant diseases.The success of these compounds has sparked intense interest and competition to develop inhibitors of chromatin modifying enzymes. Epigenetic ‘readers,’ however, have received comparatively little attention until recently.

Epigentic Readers and Bromodomains

Epigenetic readers are structurally diverse proteins each possessing one or more evolutionarily conserved effector modules, which recognize covalent modifications of histone proteins or DNA (*15*). Bromodomains are principally responsible for the context-specific molecular recognition of the ε-N-acetylation of lysine residues on histone tails (Kac) (*16-18*). There are 42 human proteins containing a total of 58 diverse bromodomains (*18*). Bromodomain-containing proteins are of substantial biological interest, as components of transcription factor complexes (TAF1, PCAF, Gcn5 and CBP) and determinants of epigenetic memory (*19*).

Structurally, bromodomains are comprised of a conserved left-handed bundle of four helices (α_Z, α_A, α_B, and α_C) with the ZA and BC loops establishing a hydrophobic pocket. Within the pocket, two tyrosines and a crucial asparagine, (corresponding to Tyr1125, Tyr1167, and Asn1168 in CREB-binding protein (CBP), for example) are highly conserved across bromodomains. Co-crystal structures of bromodomains and peptide substrates illustrate the recognition of acetyl lysine by the pocket, linked via a hydrogen bond to the asparagine residue. Aside from these crucial residues, high variability within the ZA and BC loops is responsible for binding specificity (*16-18, 20*). This finding is corroborated by the successful development of the first in class BET bromodomain inhibitor, JQ1 (described below), which utilizes shape complementarity with the bromodomain to accomplish BET family-specific binding (*21*).

The bromodomain and extra-terminal domain (BET) subfamily of bromodomains includes BRD2, BRD3 and BRD4. BET bromodomains function to facilitate cell cycle progression, establish mitotic memory, and mediate transcriptional elongation via

recruitment of the positive transcription elongation factor complex (P-TEFb; CDK9-CyclinT) (*22, 23*). In the past ten years, our lab has collaboratively characterized the role of BRD4 as a MYC-specific transcriptional co-activator in hematologic malignancies,(*24-27*) and as a NFkB-specific co-activator in inflammatory tissues (*28-30*). BRD4 functions in chromatin-dependent transmission of gene activation signals from cis-regulatory elements, or enhancers, where BRD4 localizes (*24, 27*). A therapeutic rationale for targeting BRD4 as cancer therapy has been established using the prototypical bromodomain inhibitor JQ1 from our group (*21*). In our index study on BET inhibition, we illustrated the capacity for targeted therapy in high-risk lung cancer featuring BET-rearrangement (*21*). Since publishing this work, studies in other human cancers, including multiple myeloma (REF), acute myeloid leukemia (*26*), diffuse large B cell lymphoma (*24*), acute lymphoblastic leukemia (*31*), and neuroblastoma (*32*), and a now expanded set of structurally-divergent chemical probes targeting BET bromodomains (*33*), establish a desirable translational purpose to target BRD4 in cancer. Already, drug-like derivatives of JQ1 and other structurally diverse BET bromodomain inhibitors have progressed to human clinical investigation (Clinicaltrial.gov identifier: NCT01587703, NCT01713582, NCT01949883, NCT01987362). These studies resonate with the biological hypothesis that BET bromodomains mediate chromatin-dependent regulation of gene expresion and establish a desirable translational rationale to target bromodomains in cancer.

CREB-binding Protein and Cancer

CREB-binding protein (CBP) was first isolated as a coactivator of the cAMP response element-binding (CREB) transcription factor (*34*). CBP is a 2442 amino acid-long, multi-functional protein that contains a bromodomain as well as a KIX, zinc-finger, and acetyl transferase domain (*35, 36*). CBP is highly homologous to the better-characterized bromodomain-containing protein P300, sharing 63% sequence similarity (*37*). The bromodomains of CBP and P300 are even more highly conserved. Running a BLAST sequence alignment of the human CBP bromodomain (NCBI Accession: AAC51331, amino acids 1087-1194) and the human P300 bromodomain (NCBI Accession: CAI23037, amino acids 1051-1158) shows that the two bromodomains are 97% homologous. CBP and P300 perform many of the same cellular functions and share transcription factor binding partners; although, mouse knockout studies have demonstrated that they each maintain some distinct functions (*38*). The multi-domain structure of CBP engenders it with the ability to couple a wide variety of functions, establishing it as a critical player in many major biological pathways. CBP is involved in pathways responsible for cell proliferation and growth, cellular differentiation and development, cognitive function, and cell adhesion (*39-41*).

The bromodomain of CBP is thought to be responsible for the recruitment of CBP to a variety of promoters. Although the recruitment mechanisms of CBP to promoters involved in cancer are unclear, it is generally accepted that the ability of CBP to recognize histone acetylation is a mechanism by which CBP contributes to gene regulation (*42-47*). This is founded on the observation of CBP/P300's ability to bind acetylated histone peptides *in vitro* (*20*). The bromodomain of the CBP homolog P300

has been shown to bind *in vitro* chromatin templates and isolated nucleosomes (*44, 48, 49*). Moreover, it has been demonstrated that other human bromodomains such as BRD4 bind acetylated lysines on chromatin and mediate gene expression (*19, 21*). The fact that the CBP bromodomain and acetyl transferase domain are necessary components of the MLL-CBP fusion protein to maintain its specific acute myeloid leukemia phenotype suggest that the association of CBP with chromatin is important for maintaining specific patterns of gene expression (*50, 51*).

Encoded epigenetic modifying domains enable CBP to couple transcription factor recognition to chromatin remodeling, critically mediating gene expression (*42, 46*). CBP is thought to promote gene expression in three main ways: as a bridge, as a scaffold, and as a histone acetyl transferase. Acting as a bridge, CBP localizes to transcription factors and recruits basal transcription machinery. Secondly, CBP serves as a site of nucleation for large multi-protein complexes, increasing local concentrations of transcriptional activators. Finally, CBP recruitment to a particular stretch of chromatin enables local hyperacetylation through its acetyl transferase domain, destabilizing chromatin structure and permitting transcription factors access to the DNA (*42*).

CBP functions as a transcriptional co-activator that regulates gene expression in major pathways of growth and development, such as p53 (*52*) and BCL6 (*53*). Indeed, CBP has been shown to play a critical role in the pathogenesis of cancer, particularly in hematologic diseases, and thus represents a vital mechanistic and therapeutic target. (*37, 40*). Chromosomal translocations of the CBP locus with the monocytic leukemia zinc finger (MOZ) protein and the mixed lineage leukemia (MLL) protein culminate in chimeric fusion proteins pathogenic in acute myeloid leukemia (*9, 37, 54, 55*). The MLL-

CBP fusion protein maintains the CBP bromodomain and acetyl transferase domain. Studies have demonstrated that those two domains are necessary and sufficient for myeloid proliferation when fused to MLL (*50, 51*). Moreover, in murine hematopoietic progenitor cells, transduction of MLL-CBP constructs lacking the CBP bromodomain exhibit decreased proliferative activity compared to the normal MLL-CBP construct. Here, the bromodomain could be responsible for the recruitment of specifically acetylated transcription factors or the localization of MLL-CBP to acetylated histones (*51*). Discrete somatic mutations of CBP are observed in a variety of cancers, including lung, breast, ovarian, and colon cancers (*37, 40, 56-58*). Germline mutation of CBP results in Rubinstein-Taybi syndrome (*59, 60*), which confers a greater likelihood of developing childhood malignancies (*61*). CBP can contribute to cancer even without mutation due to its involvement in other pathways that become dysregulated. For example, CBP is a member of a chromatin-remodeling complex that associates with the breast and ovarian cancer susceptibility gene *BRCA1* and thus serves as a link between chromatin remodeling to breast and ovarian cancer pathogenesis (*62, 63*). CBP is also recruited to promoters of genes such as factor VII and parathyroid hormone-related protein, which factor into tumorigenic behavior in breast cancer, where it promotes gene expression.

Lastly, small molecule inhibition of the acetyltransferase domain of CBP has reduced cellular proliferation in a variety of cancers, including melanoma (*64*), prostate cancer (*65*), and AML1-ETO-positive acute myeloid leukemia (AML) (*66*), implicating oncogenic roles for CBP/P300.

Non-BET Family Bromodomain Inhibition

Chemical probes for BRD4 have demonstrated that BET bromodomain inhibition is a viable approach to treating a number of human diseases, including cancer, inflammation, and heart failure (*67, 68*). Multiple BET inhibitors are currently being tested in human clinical trials for cancer and other human diseases. In spite of remarkable progress in the identification of chemical probes of BET bromodomain function and subsequent translation into drug molecules, there are relatively few small molecule inhibitors for non-BET bromodomains (*69, 70*).

As such, the current research has been organized around the discovery and development of inhibitors for non-BET bromodomains, and specifically for CBP. First, we developed a broad, quantitative, and high-throughput biochemical assay platform capable of evaluating the potency and selectivity of small molecule collections for x members of the bromodomain family. This assay platform was validated using known bromodomain inhibitors and then used to identify novel bromodomain inhibitors of non-BET bromodomains. Next, we aimed to target the CBP bromodomain, which is responsible for the recruitment of CBP to a variety of promoters. Since recruitment mechanisms of CBP to promoters involved in cancer are unclear, a chemical probe of bromodomain function in CBP would be critical to parsing the roles of CBP's different recruitment domains and determining the mechanism by which CBP contributes to cancer pathogenesis. We developed a suite of biochemical and cellular assays to specifically report on CBP bromodomain inhibition. Lastly, we utilized the established assay platforms to discover novel CBP inhibitors and inform iterative medicinal

chemistry, with the intended goal of developing a potent, specific CBP inhibitor capable of probing the function of the CBP bromodomain in gene regulation and cancer.

Chapter 1 References

1. A. J. Bannister, T. Kouzarides, Regulation of chromatin by histone modifications. *Cell Res* 21, 381 (Mar, 2011).
2. S. L. Berger, The complex language of chromatin regulation during transcription. *Nature* 447, 407 (May 24, 2007).
3. S. L. Schreiber, B. E. Bernstein, Signaling network model of chromatin. *Cell* 111, 771 (Dec 13, 2002).
4. R. M. Campbell, P. J. Tummino, Cancer epigenetics drug discovery and development: the challenge of hitting the mark. *The Journal of clinical investigation* 124, 64 (Jan 2, 2014).
5. C. Kandoth *et al.*, Mutational landscape and significance across 12 major cancer types. *Nature* 502, 333 (Oct 17, 2013).
6. J. Marango *et al.*, The MMSET protein is a histone methyltransferase with characteristics of a transcriptional corepressor. *Blood* 111, 3145 (Mar 15, 2008).
7. C. A. French *et al.*, BRD4 bromodomain gene rearrangement in aggressive carcinoma with translocation t(15;19). *Am J Pathol* 159, 1987 (Dec, 2001).
8. C. A. French *et al.*, BRD4-NUT fusion oncogene: a novel mechanism in aggressive carcinoma. *Cancer Res* 63, 304 (Jan 15, 2003).
9. O. M. Sobulo *et al.*, MLL is fused to CBP, a histone acetyltransferase, in therapy-related acute myeloid leukemia with a t(11;16)(q23;p13.3). *Proceedings of the National Academy of Sciences of the United States of America* 94, 8732 (Aug 05, 1997).

10. J. A. Simon, R. E. Kingston, Mechanisms of polycomb gene silencing: knowns and unknowns. *Nature reviews. Molecular cell biology* 10, 697 (Oct, 2009).
11. B. F. Chen, W. Y. Chan, The de novo DNA methyltransferase DNMT3A in development and cancer. *Epigenetics : official journal of the DNA Methylation Society* 9, 669 (May, 2014).
12. T. Hamidi, A. K. Singh, T. Chen, Genetic alterations of DNA methylation machinery in human diseases. *Epigenomics* 7, 247 (Apr, 2015).
13. H. Wu, Y. Zhang, Mechanisms and functions of Tet protein-mediated 5-methylcytosine oxidation. *Genes & development* 25, 2436 (Dec 1, 2011).
14. J. E. Bradner *et al.*, Chemical phylogenetics of histone deacetylases. *Nature Chemical Biology* 6, 238 (Mar, 2010).
15. S. D. Taverna, H. Li, A. J. Ruthenburg, C. D. Allis, D. J. Patel, How chromatin-binding modules interpret histone modifications: lessons from professional pocket pickers. *Nature structural & molecular biology* 14, 1025 (Nov, 2007).
16. S. Mujtaba, L. Zeng, M. M. Zhou, Structure and acetyl-lysine recognition of the bromodomain. *Oncogene* 26, 5521 (Aug 13, 2007).
17. D. J. Owen *et al.*, The structural basis for the recognition of acetylated histone H4 by the bromodomain of histone acetyltransferase gcn5p. *EMBO J* 19, 6141 (Nov 15, 2000).
18. L. Zeng, M. M. Zhou, Bromodomain: an acetyl-lysine binding domain. *FEBS letters* 513, 124 (Feb 20, 2002).

19. A. Dey, A. Nishiyama, T. Karpova, J. McNally, K. Ozato, Brd4 marks select genes on mitotic chromatin and directs postmitotic transcription. *Mol Biol Cell* 20, 4899 (Dec, 2009).

20. L. Zeng, Q. Zhang, G. Gerona-Navarro, N. Moshkina, M. M. Zhou, Structural basis of site-specific histone recognition by the bromodomains of human coactivators PCAF and CBP/p300. *Structure* 16, 643 (Apr, 2008).

21. P. Filippakopoulos *et al.*, Selective inhibition of BET bromodomains. *Nature* 468, 1067 (Dec 23, 2010).

22. Z. Yang *et al.*, Recruitment of P-TEFb for stimulation of transcriptional elongation by the bromodomain protein Brd4. *Molecular cell* 19, 535 (Aug 19, 2005).

23. M. K. Jang *et al.*, The bromodomain protein Brd4 is a positive regulatory component of P-TEFb and stimulates RNA polymerase II-dependent transcription. *Molecular cell* 19, 523 (Aug 19, 2005).

24. B. Chapuy *et al.*, Discovery and characterization of super-enhancer-associated dependencies in diffuse large B cell lymphoma. *Cancer cell* 24, 777 (Dec 9, 2013).

25. J. E. Delmore *et al.*, BET bromodomain inhibition as a therapeutic strategy to target c-Myc. *Cell* 146, 904 (Sep 16, 2011).

26. J. Zuber *et al.*, RNAi screen identifies Brd4 as a therapeutic target in acute myeloid leukaemia. *Nature* 478, 524 (Dec 16, 2011).

27. J. Loven *et al.*, Selective inhibition of tumor oncogenes by disruption of super-enhancers. *Cell* 153, 320 (Apr 11, 2013).

28. J. D. Brown *et al.*, NF-kappaB directs dynamic super enhancer formation in inflammation and atherogenesis. *Molecular cell* 56, 219 (Oct 23, 2014).

29. B. Huang, X. D. Yang, M. M. Zhou, K. Ozato, L. F. Chen, Brd4 coactivates transcriptional activation of NF-kappaB via specific binding to acetylated RelA. *Molecular and cellular biology* 29, 1375 (Mar, 2009).

30. E. Nicodeme *et al.*, Suppression of inflammation by a synthetic histone mimic. *Nature* 468, 1119 (Dec 23, 2010).

31. C. J. Ott *et al.*, BET bromodomain inhibition targets both c-Myc and IL7R in high-risk acute lymphoblastic leukemia. *Blood* 120, 2843 (Oct 4, 2012).

32. A. Puissant *et al.*, Targeting MYCN in Neuroblastoma by BET Bromodomain Inhibition. *Cancer Discovery* 3, 308 (Mar 1, 2013).

33. M. Tanaka, J. M. Roberts, J. Qi, J. E. Bradner, Inhibitors of emerging epigenetic targets for cancer therapy: a patent review (2010-2014). *Pharmaceutical patent analyst* 4, 261 (Jul, 2015).

34. R. P. Kwok *et al.*, Nuclear protein CBP is a coactivator for the transcription factor CREB. *Nature* 370, 223 (Jul 21, 1994).

35. R. H. Giles *et al.*, Detection of CBP rearrangements in acute myelogenous leukemia with t(8;16). *Leukemia* 11, 2087 (Dec, 1997).

36. M. Delvecchio, J. Gaucher, C. Aguilar-Gurrieri, E. Ortega, D. Panne, Structure of the p300 catalytic core and implications for chromatin targeting and HAT regulation. *Nature structural & molecular biology* 20, 1040 (Sep, 2013).

37. N. G. Iyer, H. Ozdag, C. Caldas, p300/CBP and cancer. *Oncogene* 23, 4225 (May 24, 2004).

38. A. L. Kung *et al.*, Gene dose-dependent control of hematopoiesis and hematologic tumor suppression by CBP. *Genes & development* 14, 272 (Feb 01, 2000).

39. J. E. Eid, A. L. Kung, R. Scully, D. M. Livingston, p300 interacts with the nuclear proto-oncoprotein SYT as part of the active control of cell adhesion. *Cell* 102, 839 (Sep 15, 2000).

40. R. H. Goodman, S. Smolik, CBP/p300 in cell growth, transformation, and development. *Genes & development* 14, 1553 (Jul 01, 2000).

41. S. Trompet *et al.*, Variation in the CBP gene involved in epigenetic control associates with cognitive function. *Neurobiol Aging* 32, 549 e1 (Mar, 2011).

42. H. M. Chan, N. B. La Thangue, p300/CBP proteins: HATs for transcriptional bridges and scaffolds. *J Cell Sci* 114, 2363 (Jul, 2001).

43. G. A. Blobel, CBP and p300: versatile coregulators with important roles in hematopoietic gene expression. *J Leukoc Biol* 71, 545 (Apr, 2002).

44. Z. Deng *et al.*, The CBP bromodomain and nucleosome targeting are required for Zta-directed nucleosome acetylation and transcription activation. *Molecular and cellular biology* 23, 2633 (Apr, 2003).

45. N. Champagne, N. Pelletier, X. J. Yang, The monocytic leukemia zinc finger protein MOZ is a histone acetyltransferase. *Oncogene* 20, 404 (Jan 18, 2001).

46. E. Kalkhoven, CBP and p300: HATs for different occasions. *Biochem Pharmacol* 68, 1145 (Sep 15, 2004).

47. H. Fukuda, N. Sano, S. Muto, M. Horikoshi, Simple histone acetylation plays a complex role in the regulation of gene expression. *Brief Funct Genomic Proteomic* 5, 190 (Sep, 2006).

48. E. T. Manning, T. Ikehara, T. Ito, J. T. Kadonaga, W. L. Kraus, p300 forms a stable, template-committed complex with chromatin: role for the bromodomain. *Molecular and cellular biology* 21, 3876 (Jun, 2001).

49. A. Ragvin *et al.*, Nucleosome binding by the bromodomain and PHD finger of the transcriptional cofactor p300. *J Mol Biol* 337, 773 (Apr 02, 2004).

50. C. Lavau, C. Du, M. Thirman, N. Zeleznik-Le, Chromatin-related properties of CBP fused to MLL generate a myelodysplastic-like syndrome that evolves into myeloid leukemia. *EMBO J* 19, 4655 (Sep 01, 2000).

51. D. A. Santillan *et al.*, Bromodomain and histone acetyltransferase domain specificities control mixed lineage leukemia phenotype. *Cancer Res* 66, 10032 (Oct 15, 2006).

52. W. Gu, X. L. Shi, R. G. Roeder, Synergistic activation of transcription by CBP and p53. *Nature* 387, 819 (Jun 19, 1997).

53. O. R. Bereshchenko, W. Gu, R. Dalla-Favera, Acetylation inactivates the transcriptional repressor BCL6. *Nat Genet* 32, 606 (Dec, 2002).

54. J. Borrow *et al.*, The translocation t(8;16)(p11;p13) of acute myeloid leukaemia fuses a putative acetyltransferase to the CREB-binding protein. *Nat Genet* 14, 33 (Sep, 1996).

55. G. Yang *et al.*, Epigenetic regulation of tumor suppressors in t(8:21)-containing AML. *Ann Hematol* 83 Suppl 1, S83 (2004).

56. Y. Ionov, S. Matsui, J. K. Cowell, A role for p300/CREB binding protein genes in promoting cancer progression in colon cancer cell lines with microsatellite instability. *Proceedings of the National Academy of Sciences of the United States of America* 101, 1273 (Feb 03, 2004).

57. M. Kishimoto *et al.*, Mutations and deletions of the CBP gene in human lung cancer. *Clin Cancer Res* 11, 512 (Jan 15, 2005).

58. R. Ward, M. Johnson, V. Shridhar, J. van Deursen, F. J. Couch, CBP truncating mutations in ovarian cancer. *J Med Genet* 42, 514 (Jun, 2005).

59. F. Petrij *et al.*, Rubinstein-Taybi syndrome caused by a De Novo reciprocal translocation t(2;16)(q36.3;p13.3). *Am J Med Genet* 92, 47 (May 01, 2000).

60. F. Petrij *et al.*, Rubinstein-Taybi syndrome caused by mutations in the transcriptional co-activator CBP. *Nature* 376, 348 (Jul 27, 1995).

61. R. W. Miller, J. H. Rubinstein, Tumors in Rubinstein-Taybi syndrome. *Am J Med Genet* 56, 112 (Mar 13, 1995).

62. D. A. Bochar *et al.*, BRCA1 is associated with a human SWI/SNF-related complex: linking chromatin remodeling to breast cancer. *Cell* 102, 257 (Jul 21, 2000).

63. G. M. Pao, R. Janknecht, H. Ruffner, T. Hunter, I. M. Verma, CBP/p300 interact with and function as transcriptional coactivators of BRCA1. *Proceedings of the National Academy of Sciences of the United States of America* 97, 1020 (Feb 01, 2000).

64. D. Bandyopadhyay *et al.*, Down-regulation of p300/CBP histone acetyltransferase activates a senescence checkpoint in human melanocytes. *Cancer Res* 62, 6231 (Nov 01, 2002).

65. F. R. Santer *et al.*, Inhibition of the acetyltransferases p300 and CBP reveals a targetable function for p300 in the survival and invasion pathways of prostate cancer cell lines. *Mol Cancer Ther* 10, 1644 (Sep, 2011).

66. X. N. Gao *et al.*, A histone acetyltransferase p300 inhibitor C646 induces cell cycle arrest and apoptosis selectively in AML1-ETO-positive AML cells. *PLoS One* 8, e55481 (2013).

67. J. Shi *et al.*, Disrupting the interaction of BRD4 with diacetylated Twist suppresses tumorigenesis in basal-like breast cancer. *Cancer cell* 25, 210 (Feb 10, 2014).

68. Y. H. Wang *et al.*, BRD4 promotes pancreatic ductal adenocarcinoma cell proliferation and enhances gemcitabine resistance. *Oncol Rep* 33, 1699 (Apr, 2015).

69. R. Sanchez, J. Meslamani, M. M. Zhou, The bromodomain: from epigenome reader to druggable target. *Biochim Biophys Acta* 1839, 676 (Aug, 2014).

70. F. M. Ferguson *et al.*, Targeting low-druggability bromodomains: fragment based screening and inhibitor design against the BAZ2B bromodomain. *J Med Chem* 56, 10183 (Dec 27, 2013).

Chapter 2

Development of Assays for Studying CBP Inhibition

Contributers: Katharin Shaw, Jun Qi, Michael McKeown, Rhamy Zeid, Sarah Vittori-Winter, Jason Marineau, Roodolph St. Pierre, Andrew Alexander

Introduction

Toward the over-arching goal of developing inhibitors for the CREB-binding protein (CBP), biochemical and cellular assays have been developed to assess compound efficacy. The AlphaScreen assay was utilized for the biochemical binding assay due to its robust, high-throughput nature. Moreover, this assay format is well suited to assess bromodomain-inhibitor binding, as previously demonstrated by the successful implementation of BRD4 and BRDT AlphaScreen assays (*1*). These bromodomain assays developed in the Bradner Lab in parallel provided a means for quickly counterscreening in order to establish selectivity and eliminate promiscuous binders.

Cellular assays were implemented with the goal of assessing whether the chemical inhibition of the CBP bromodomain affected cellular function. In order to establish the target engagement of small molecule inhibitors, a novel assay was developed that could definitively determine whether compounds could engage the CBP protein in a cellular context. A bioluminescence resonance energy transfer (BRET) assay was chosen for this role. This assay has theoretical advantages over fluorescence resonance energy transfer (FRET) or fluorescence recovery after photobleaching (FRAP) assays in its dynamic range and throughput. However, this assay does not report on the biological impact of CBP bromodomain inhibition, nor is it well-suited to measuring multiple dose points for a large number of compounds. Therefore, cellular viability assays, which can be miniaturized and automated, were incorporated into this assay platform as a means of compound testing on a large-scale

in dose response. This cellular assay reports on viability through the measurement of the total ATP content of each well in an assay plate. Due to the nature of the readout, this assay does not differentiate between various anti-proliferative mechanisms and is not pathway-specific with off-target effects possibly impacting results.

All together, this CBP assay platform engenders the discovery and development of CBP inhibitors, ensuring that these compounds engage CBP in a cellular context and providing a basis for future medicinal chemistry toward the goal of developing chemical probes to further decipher the role of CBP bromodomain in cancer, which can be further pursued for cancer therapy.

Development of a robust high-throughput assay for detecting CBP inhibition

Description and development of AlphaScreen assay

With the goal of developing a chemical probe that potently and selectively targets the CBP bromodomain, I have exploited AlphaScreen technology to develop and optimize a primary assay capable of evaluating and characterizing the binding of small molecules to the CBP bromodomain. AlphaScreen (**A**mplified **L**uminescent **P**roximity **H**omogenous **A**ssay Screen) is a homogenous luminescence assay capable of reporting on protein-protein interactions inferred through proximity. The assay is adaptable to high-throughput screening and is capable of yielding inhibition results in dose response. This assay is chosen over comparable assays such as fluorescence resonance energy transfer (FRET) and fluorescence polarization (FP) and other reverse chemical genetic screens for a variety of reasons. Because AlphaScreen donor and acceptor bead interactions are avid, the assay requires much less protein to maintain high signal and exhibit a more dramatic dynamic range. Unlike fluorescent assays, AlphaScreen produces an anti-Stokes shift, reducing the confounding effect intrinsically fluorescent molecules could have in an assay. This assay has an advantage over FRET in that the restrictions of molecular orientation and proximity that affect FRET are loosened. Interaction between donor and acceptor in AlphaScreen can take place over 200 nm instead of 10 nm and do not require a specific orientation. Finally, AlphaScreen does not require any alterations to the small molecules being screening, presenting an advantage over assay that require tethering, such as microarrays.

In the case of my primary screening assay, it reports on the CBP bromodomain-H3K56Ac binding event. Through the execution of micro-SPOT arrays of a variety of bromodomains against common acetylated histone peptides, our collaborators at the Structural Genomics Consortium have observed that the CBP bromodomain binds to H3K56Ac, H3K36Ac, H3K27Ac, and H4K44Ac *in vitro* (*2*). H3K56Ac was chosen as the ligand for the assay because of its binding efficacy and biological relevance (*3*). The H3K56Ac peptide was synthesized on the Liberty CEM Microwave Peptide Synthesizer using the sequence N'-IRRYQKSTELL-C'. The peptide was subsequently acetylated at the lysine, biotinylated, cleaved, and purified. Recombinant, human his_6-CBP bromodomain was initially obtained by collaborators at the SGC, then produced in-house following their protein expression and purification protocols (*4*).

This assay is miniaturized and yields robust CBP- and H3K56Ac-dependent signal. The assay is comprised of his_6-CBP bromodomain bound to a Ni^{++} acceptor bead and biotinylated H3K56Ac bound to a streptavidin donor bead. The excitation of donor beads by 640 nm light generates singlet molecular oxygen, which can traverse a distance of approximately 200 nm over the lifetime of its excited state. If the acceptor beads are in close proximity, the singlet molecular oxygen triggers a chemical cascade within the acceptor beads, ultimately resulting in a luminescent emission at 570 nm. The interaction of the CBP bromodomain and H3K56Ac bring the two bead types into close proximity, yielding luminescent signal (Figure 2.1A); inhibition of the protein-ligand association results in signal attenuation (*5*).

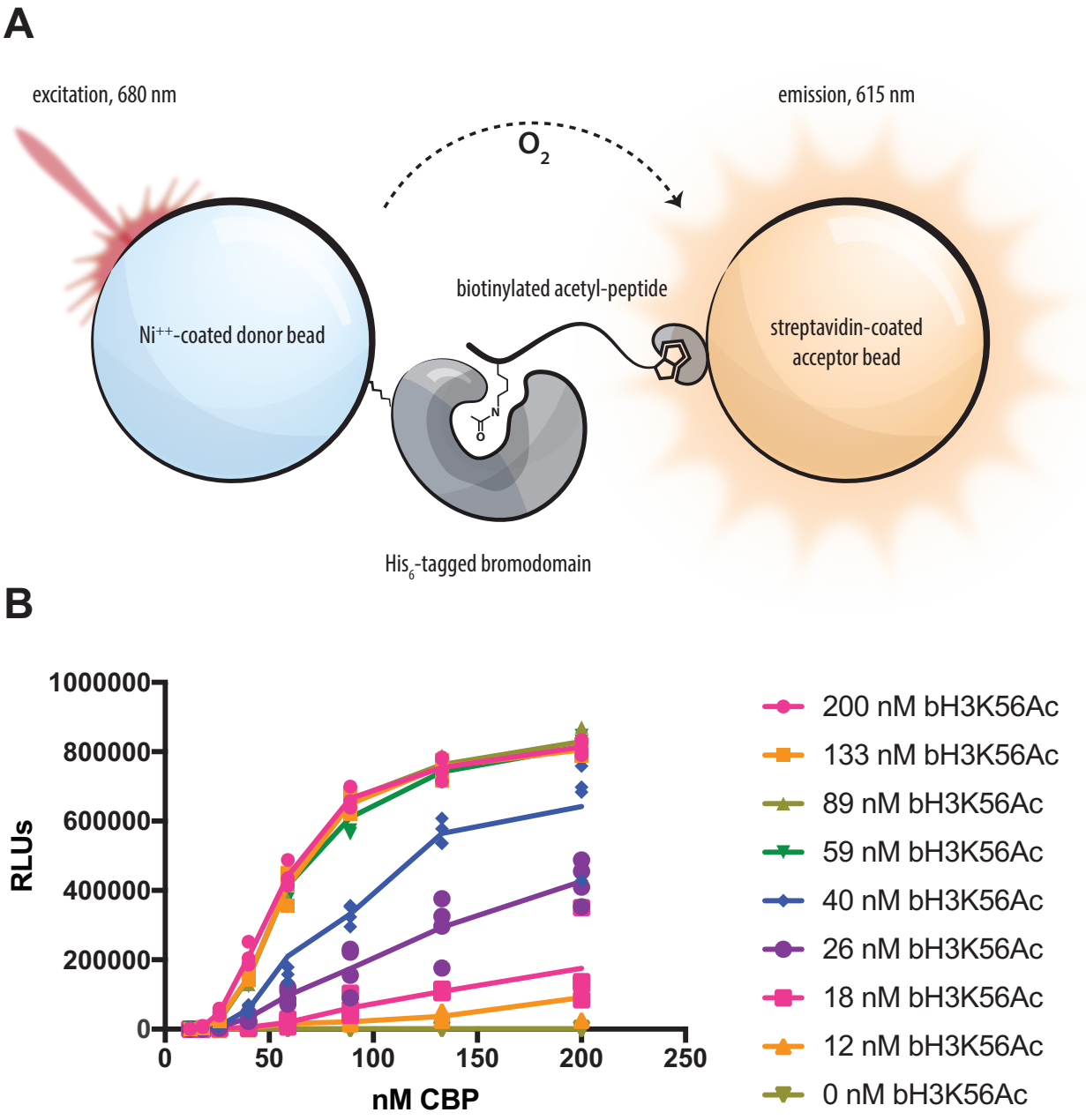

Figure 2.1 Biochemical Assay for Evaluating CBP Inhibition (A) Diagram of AlphaScreen assay showing the bromodomain-acetyllysine binding event. Biotinylated peptide is bound to streptavidin-coated acceptor bead, and His_6-tagged bromodomain binds to Ni^{++}-coated donor bead **(B)** AlphaScreen assay optimization. The assay is performed with varying bromodomain and biotinylated peptide concentrations

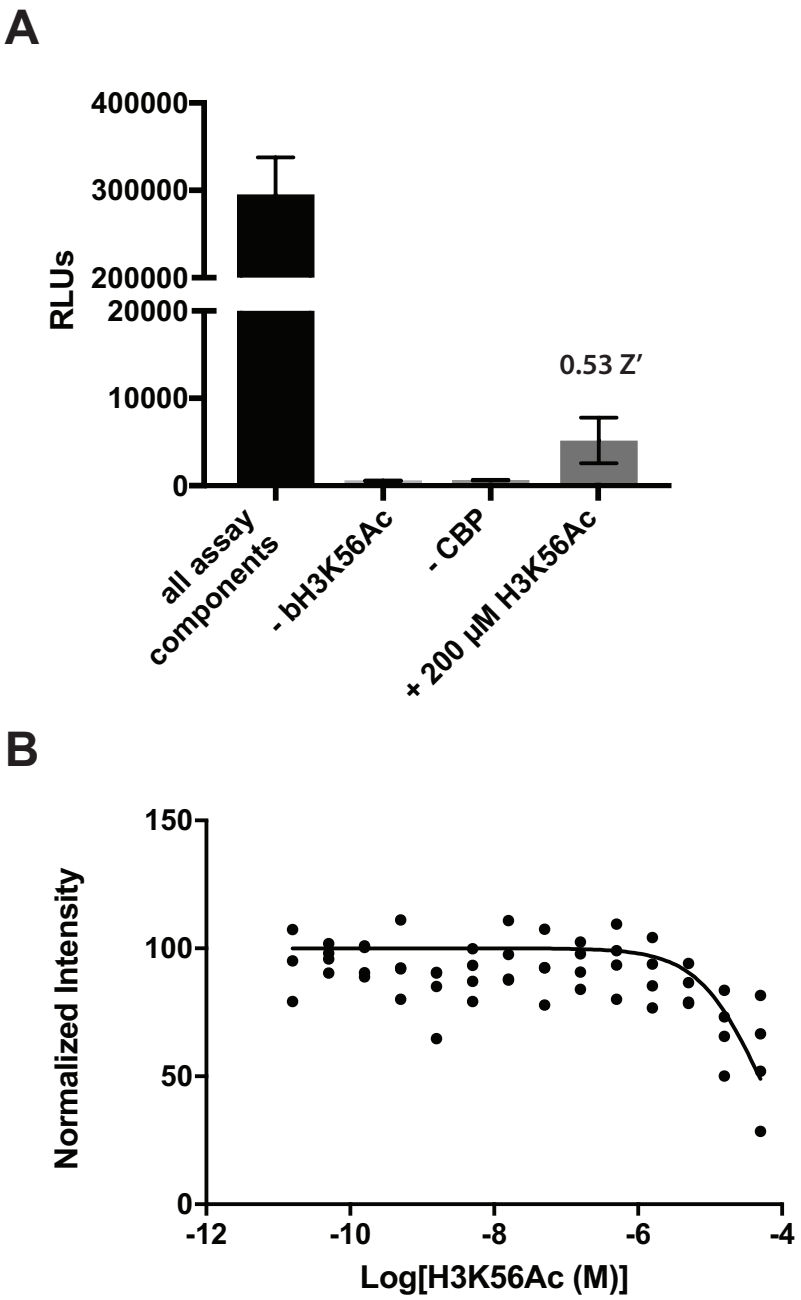

Figure 2.2 CBP AlphaScreen Assay Performance (A) 33 replicates of each condition show assay signal with full complement of assay components, biotinylated peptide dropout, protein dropout, and the addition of free peptide to the assay. Z' of 0.53 using 200 µM of free H3K56Ac peptide demonstrates suitability of assay for screening **(B)** 14-point dose response of free H3K56Ac peptide demonstrates signal attenuation with inhibition

In order to optimize signal and inhibition response and minimize background, a matrix of conditions, varying both protein and ligand concentrations (including drop-outs), was evaluated while maintaining constant bead concentrations in a reaction buffer (Figure 2.1B). This reaction buffer (50 mM HEPES, 150 mM NaCl, 0.1% w/v BSA, 0.01% v/v Tween-20, pH 7.4) was formulated to approximate cellular salinity and pH and included detergent and BSA to minimize background noise and nonspecific interactions. This optimization is performed with subsequent batches of protein and ligand to ensure assay efficiency. A Z' assay was performed to assess assay robustness and reported a Z' factor of 0.53, indicating its suitability for compound screening (Figure 2.2A). Using a non-biotinylated H3K56Ac peptide as a positive control, this assay was performed in 10-point dose response to demonstrate that the AlphaScreen assay yields an IC50 with good fit (Figure 2.2B).

Troubleshooting problems upon introduction of compound

Unlike other bromodomain assays, such as the BET-subfamily bromodomain AlphaScreen assays established in our lab, AlphaScreen assays with CBP performed less reliably. The CBP bromodomain is much less stable in assay buffer over time, and signal varied wildly with changes in thawed aliquot under the same assay conditions. Whereas BET bromodomains remain stable in assay buffer at 4°C for up to a month, CBP becomes unusable after approximately 3-4 hours. By adding 500 μM of the reducing agent dithiothreitol (DTT) to the acceptor bead mix containing protein, the assay consistently produces signal (Figure 2.3A).

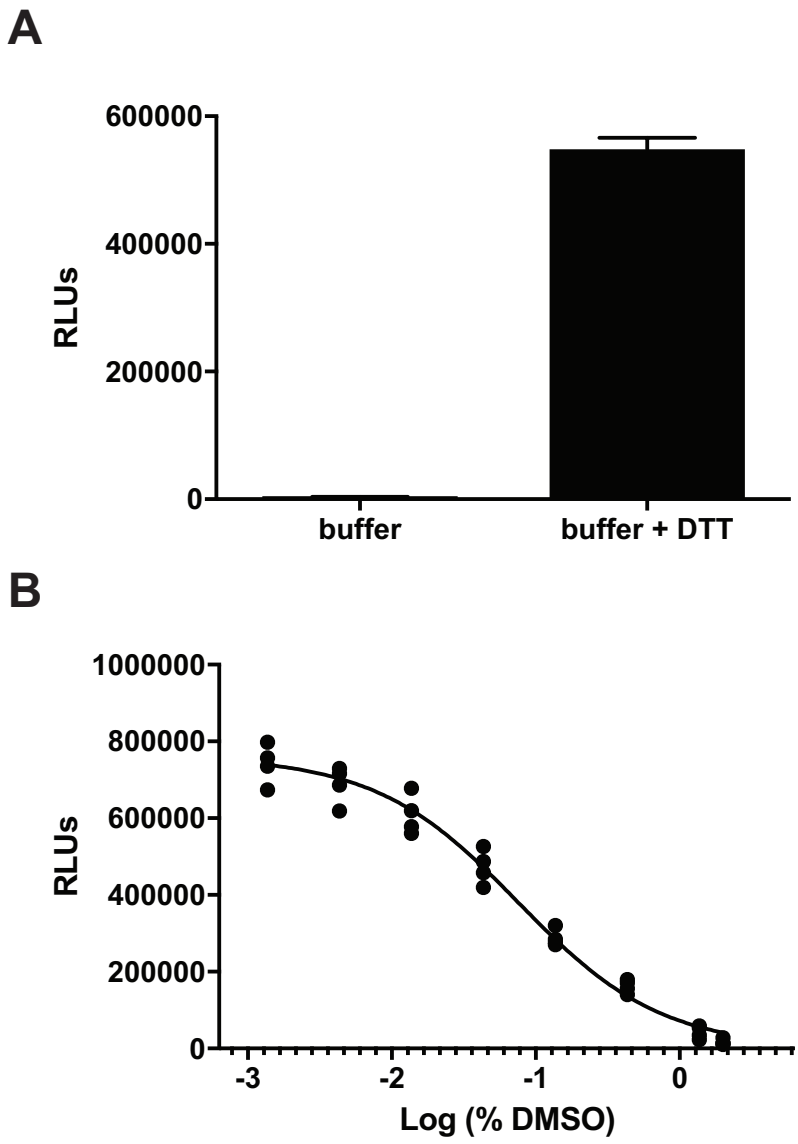

Figure 2.3 CBP AlphaScreen Assay Troubleshooting (A) Assay signal with and without reducing agent DTT added to reaction buffer **(B)** Titration of assay with DMSO shows CBP inhibition

While including DTT in the assay yielded reliable signal, it was challenging to obtain logistic regression curves from dose response data due to erratic patterns of inhibition. The only difference between the assay that worked with H3K56Ac and assays performed with pin-transferred compounds was the presence of DMSO. To test the hypothesis that assay variability was due to DMSO, a titration was performed, and the result indicated a decline in robust and stable signal with increasing DMSO concentrations, suggesting that the CBP bromodomain is inhibited by DMSO (Figure 2.3B). Moreover, studies performed by our collaborators at the SGC in Oxford demonstrated CBP crystallizes with DMSO.

This DMSO sensitivity precluded the pin transfer of compounds into the low volumes employed in 384-well plates. In order to account for DMSO inhibition, compounds (10 mM in DMSO) were serially diluted into assay buffer by hand, and the signal was normalized to the corresponding concentration of DMSO in the control. While performing the assay in this manner yielded signal, the method was not conducive to high-throughput screening. I then adapted the assay to eliminate the necessity of non-automated steps and reduce the number of liquid handling steps, thus accommodating the screening of larger compound collections. Compound plates were pinned into 384-well AlphaPlates containing 40 ul of ethanol. The AlphaPlates were placed in a vacuum desiccator for no shorter than 48 hours, effectively removing the DMSO along with the ethanol. A 10 uL solution of CBP bromodomain (200 nM final), biotin-H3K56Ac (200 nM final), and Ni^{++}-coated acceptor bead (25 µg/ml final) were added to the plate with a BioTek EL406 liquid handler. Following a 30 minute incubation on a plate shaker, a 10 ul solution of streptavidin-coated donor bead was added to the

plate. AlphaScreen measurements were taken using manufacturer's protocol on a PerkinElmer Envision 2104 after 1 hour. Experiments performed using assay-ready plates consistently yielded reliable dose response curves, except in the case of compounds that proved to be insoluble in the reaction buffer. A series of triazolophthalazine compounds, which collaborators found to inhibit CBP in thermal shift assays, were used to establish assay success (Figure 2.4).

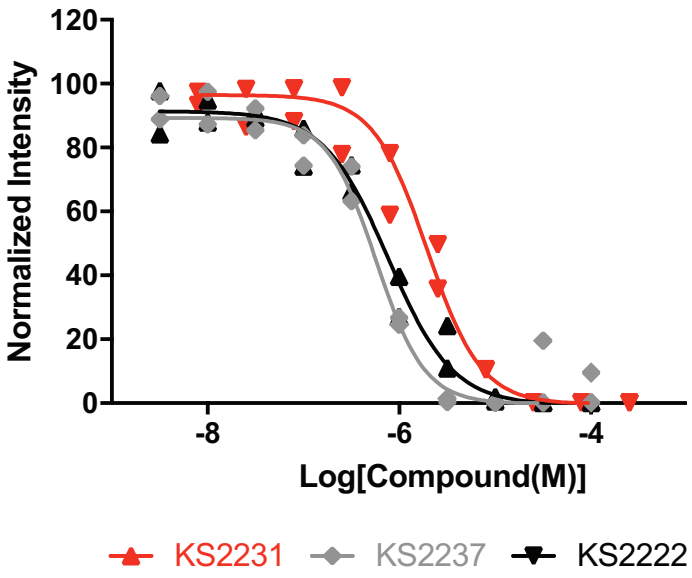

Figure 2.4 AlphaScreen Assay Using Assay Ready Plates Dose response of three triazolophthalazine compounds in AlphaScreen assay shows successful implementation of assay ready plates

Development of an assay to detect cellular engagement of CBP

Establishing and troubleshooting assay

In parallel, I have been working on means to directly assess CBP target engagement in a cellular system. Toward this goal, I have been optimizing a BRET assay. BRET is an energy transfer-based proximity assay, enabling the direct study of protein-protein interactions in living cells. It yields improvements over the similar fluorescence resonance energy transfer (FRET) assay since there is no need for an external excitation light source, generally resulting in lower background. The CBP BRET assay measures the effect of CBP bromodomain inhibition on the interaction of CBP and chromatin in a miniaturized 96-well plate format. The assay is comprised of histone 3-HaloTag (H3-HT) which covalently binds to a chloro-alkane on tetramethylrhodamine (TMR), NanoLuciferase (NL)-tagged CBP, and NanoGlo substrate. Light emitted from the luciferase reaction excites the dye TMR when CBP and H3 are in proximity, resulting in signal attenuation with increasing inhibition (Figure 2.5).

The methods involved in executing this assay include a lipid-based co-transfection of H3-HT and NL-tagged CBP plasmids, transfer to 96-well assay plates, treatment with inhibitors and vehicle, and the addition of TMR ligand and NanoGlo substrate prior to reading signal at 450 and 610 nm. The TMR emission is normalized to cell count in each well by dividing 610 nm readouts by 450 nm readouts, and background noise is assessed by analyzing 610/450 nm readout when no TMR is added.

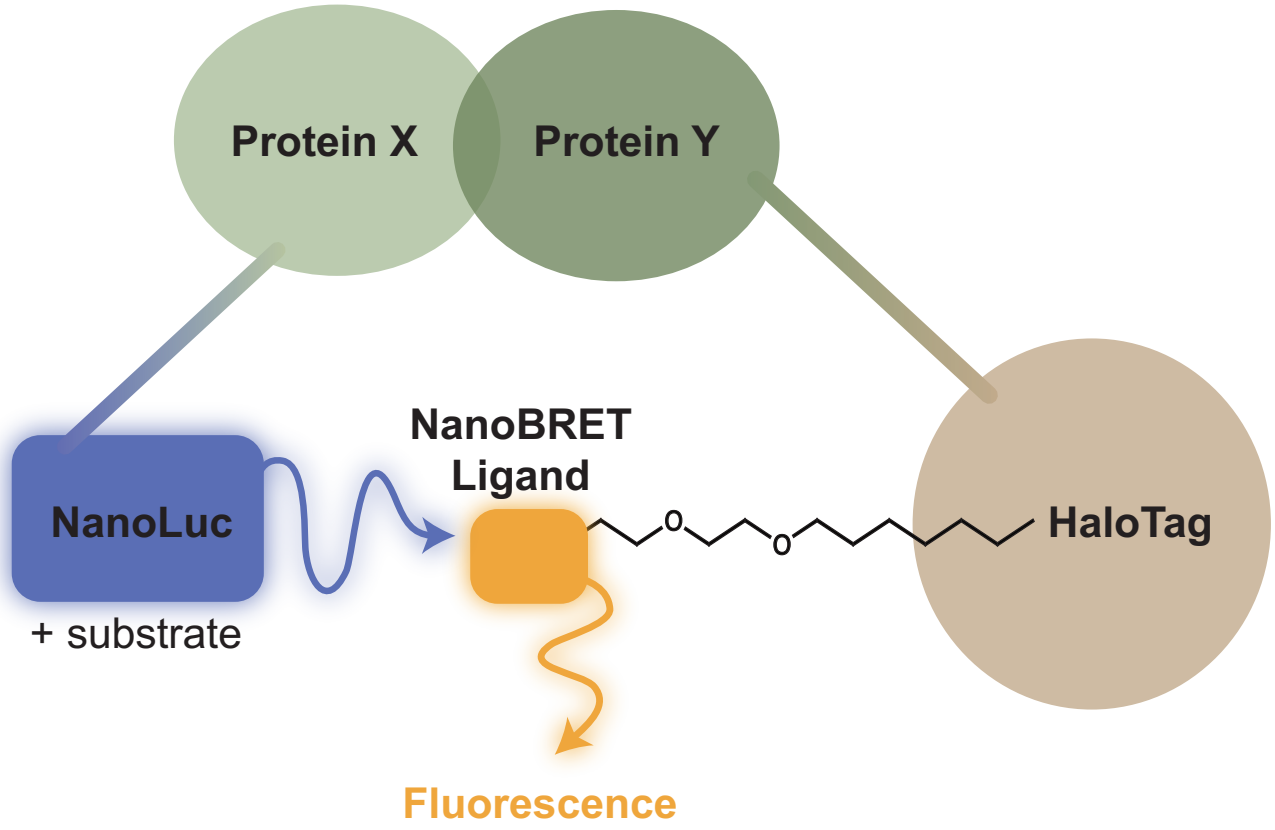

Figure 2.5 BRET Assay Schematic Diagram of assay showing Protein X bound to NanoLuciferase and Protein Y bound to HaloTag, which attaches to a NanoBRET Ligand (e.g. TMRDirect) by means of a chloro-alkane

In this target engagement assay, CBP bromodomain and histone acetyltransferase domain, and full-length CBP in order to understand whether CBP inhibitors disrupt the acetyllysine-bromodomain recognition event in a cellular system. Provided that inhibitors engage the bromodomain in cells, is bromodomain inhibition able to disrupt CBP-histone interaction when more domains of CBP need to be disassociated from chromatin as well?

I first attempted to establish the bromodomain only assay as a means of validating cellular target engagement. Various transfection ratios and time points were evaluated in order to optimize the assay; however, high day-to-day variability in assay performance occurred even with optimized conditions. There existed high background signal and low TMR-generated 450 nm emission; moreover, low 610 nm emission indicated poor cell viability over the course of the assay. In collaboration with colleagues within the Bradner laboratory and at Promega, I optimized each of the conditions to improve assay performance.

To reduce background as much as possible, all media used in culturing cells intended for the BRET assay were phenol red-free to minimize the impact that residual phenol red could have on 450 nm emission. Low cell viability, as indicated by inconsistent or low 610 nm readout, was ameliorated by switching transfection reagents from Promega's FuGENE 6 to Clontech's XFect and by increasing the amount of time that cells settle after plating steps to 24 hours. More cells survived the co-transfection, and this ultimately resulted in more consistent 96-well plating as well as higher signal. Under advisement from the Promega Functional Proteomics team led by Dr. Danette

Daniels, we began using their proprietary TMRDirect ligand and purchased the advised mirrors and filters for the Envision plate reader used to measure signal, changing readings from 450 nm to 460 nm and from 610 nm to 595 nm. After making these adjustments, I began optimizing transfection ratios again.

I performed a donor saturation assay involving a series of double transfections, varying amounts of NL-tagged CBP bromodomain with 2 µg of H3-HT, in order to find an amount of NL-CBP_{BD} that would yield high signal still in the dynamic range of the donor saturation curve (*6*). With increasing acceptor/donor ratio, signal predictably increased; however, a discernable plateau was not reached due to extremely high variability at higher accepter/donor ratios (Figure 2.6A). The assay was performed again, focusing on the range that was most dynamic in the first experiment (Figure 2.6B). The assay still did not yield a smooth saturation curve. Rather than performing the experiment again, I chose 15 ng of NL-CBP_{BD} (A/D ratio of 133) to use in the BRET assay, as it lies in the dynamic range of both saturation curve experiments to generate preliminary assay data.

In the preliminary BRET experiment, I chose to test four compounds at two doses, including the literature reported CBP bromodomain inhibitor from the SGC {Hay, 2014 #150 (Figure 2.7). The signal over background for this assay was approximately 2-fold for the vehicle control. Both 10 µM and 500 nM conditions differed significantly from the DMSO-treated cells. These results indicate the successful development of an assay capable of reporting inhibitor engagement of the CBP bromodomain in a cellular

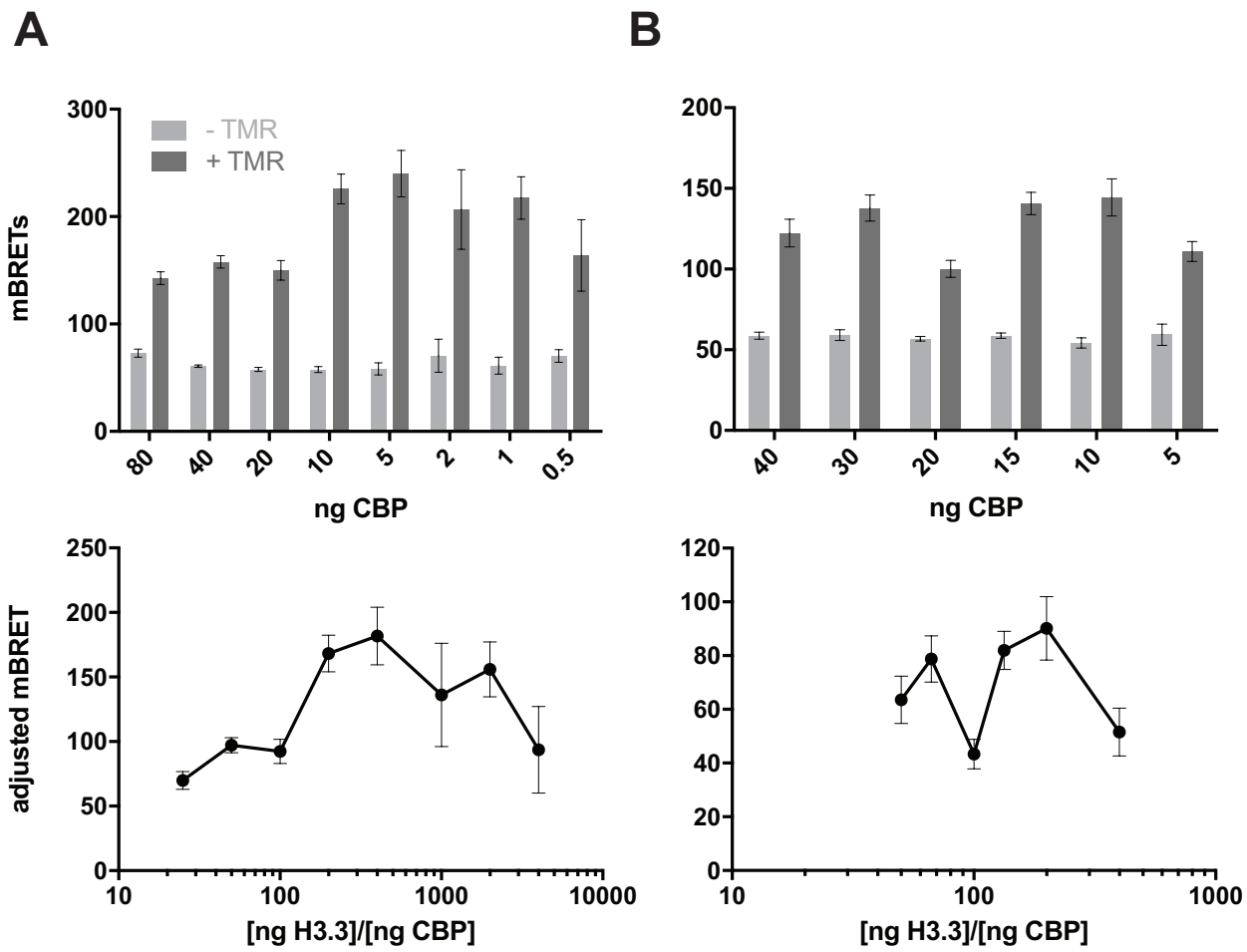

Figure 2.6 CBP Bromodomain BRET Optimization (A) Donor saturation assay with varying NanoLuciferase-tagged CBP bromodomain. Amounts ranging from 0.5 ng to 80 ng. Above shows assay signal in mBRETs (595/460 nm emission ratio multiplied by 1000) with and without TMR for each condition. Below shows mBRET signal with TMR(-) background subtracted as a function of acceptor/donor ratio **(B)** Same as in (A), except the tested conditions are expanded in the 5 to 40 ng range of CBP bromodomain

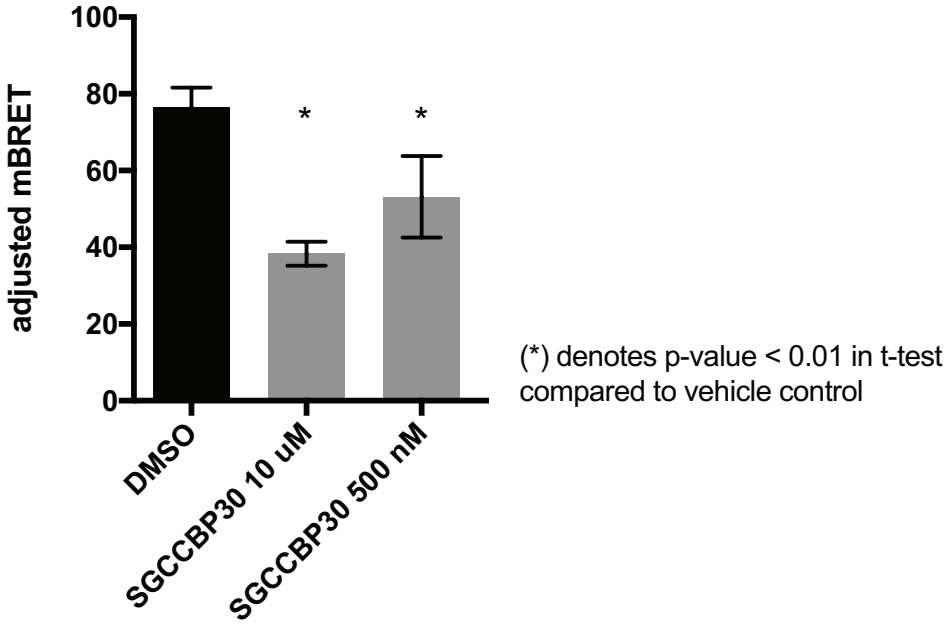

Figure 2.7 Effect of CBP inhibition on BRET signal Inhibition of the CBP bromodomain with both 10 μM and 500 nM of literature reported SGCCBP30 cause statistically significant signal attenuation.

context. Moreover, the BRET assay is sensitive to bromodomain inhibition at both high and low doses of compound treatment.

Assay protocol

Unless otherwise noted, daily steps are executed 24 hours apart. On Day 1, 600,000 293T cells/well in 2 ml are seeded onto a 6-well dish using phenol red-free DMEM with 10% FBS as culture media. On Day 2, 2 µg of halo-tagged histone 3 and 15 ng of nanoluciferase-tagged CBP bromodomain are diluted in Xfect Reaction buffer to a final volume of 100 µl, to which 1.5 µl of Xfect Polymer is added. The mixture is vortexed vigorously for 10 seconds, spun down briefly, and incubated at room temperature for 15 minutes. This solution is added dropwise to cells. On Day 3, cells are washed and trypsinized with phenol red-free trypsin, spun down, and resuspended in fresh culture media to be counted. Cells are split into two aliquots with a concentration of 100,000 cells/ml. TMRDirect ligand is added to one aliquot. White 96-well PerkinElmer CulturPlates are seeded with 100 µl/well. On Day 4, compounds are added performed for necessary treatment duration. After treatment is concluded, plates are removed from the incubator while a 1:600 dilution of Nano-Glo substrate in culture media is prepared. 100 µl is added to each well and incubated for 5-10 minutes. Using a PerkinElmer Envision plate reader equipped with Luminescence mirror/ Umbelliferone 460 emission filter and BODIPY TMR mirror/Cy3 595 emission filter, luminescence and TMR signal are respectively read. To calculate BRET signal, TMR signal is divided by luciferase signal.

Cellular models of CBP inhibition: CBP fusion proteins/ leukemia

In conjunction with selectivity studies, cellular viability assays can inform iterative medicinal chemistry to yield a potent, selective, cell-permeable chemical probe. Moreover, they are a means of assessing the biological outcome of bromodomain perturbation. The cellular viability assays will inform on cellular IC_{50} values and *in vivo* specificity for the CBP bromodomain. The studies are performed in 384-well format at 10-point dose response. Compounds are incubated with the cells for three days prior to reading. On the day of the readout, ATPlite (PerkinElmer) reagent—a mixture containing luciferase, luciferin, and detergent—are added to the plates to measure the ATP content of each well. After 15 minutes, the Envision reads luminescence. Since ATP is present in metabolically active cells and not in cells that have undergone necrosis or apoptosis, the measurement of ATP serves as an indicator of cell proliferation, arrest, or death. The benefit of using this assay is that it can be performed on a variety of cell lines without necessitating complex optimization. The assay is miniaturized, robust, and can be performed in high-throughput. However, since the cellular assays using ATP as a measure of viability do not differentiate between cytocidal, cytostatic, or differentiation-based mechanisms of anti-proliferative effect, an alternate method of analyzing cell growth would required to further investigate the mechanism by which bromodomain inhibition reduces viability. More intensive experiments such as flow cytometry can monitor cell count, mitotic state, and apoptosis using a fluorescent antibody against annexin V and propidium idodide.

Several leukemia lines were chosen to perform these assays, including an MLL-CBP translocation-driven acute myeloid leukemia, SN-1 (*7*). The downregulation of MLL-CBP is associated with the differentiation of the SN-1 cell line (*8*). It is expected that lower endogenous levels of MLL-CBP will decrease the transcription of the oncoprotein's target genes. Thus, inhibiting the association of MLL-CBP with chromatin should also induce differentiation, causing treated SN-1 cells to grow more slowly and produce less ATP per well compared to untreated SN-1 cells and other leukemia lines less directly dependent on CBP/P300 transcription factor function. Other lines chosen include Monomac 6, an MLL-AF9 acute monocytic leukemia (*9*), intended as a counterpoint to the SN-1's MLL-CBP translocation, as well as two other acute myeloid leukemia lines KG-1 and HL-60 (*10-12*), to further verify that the intended probes are not generally cytotoxic and act specifically on CBP-dependent leukemia.

References

1. P. Filippakopoulos *et al.*, Selective inhibition of BET bromodomains. *Nature*, (Sep 24, 2010).
2. P. Filippakopoulos *et al.*, Histone recognition and large-scale structural analysis of the human bromodomain family. *Cell* **149**, 214 (2012).
3. C. Das, M. S. Lucia, K. C. Hansen, J. K. Tyler, CBP/p300-mediated acetylation of histone H3 on lysine 56. *Nature* **459**, 113 (May 07, 2009).
4. D. A. Hay *et al.*, Discovery and optimization of small-molecule ligands for the CBP/p300 bromodomains. *Journal of the American Chemical Society* **136**, 9308 (Jul 02, 2014).
5. J. B. Baell, G. A. Holloway, New substructure filters for removal of pan assay interference compounds (PAINS) from screening libraries and for their exclusion in bioassays. *J Med Chem* **53**, 2719 (Apr 8, 2010).
6. C. Couturier, B. Deprez, Setting Up a Bioluminescence Resonance Energy Transfer High throughput Screening Assay to Search for Protein/Protein Interaction Inhibitors in Mammalian Cells. *Frontiers in endocrinology* **3**, 100 (2012).
7. Y. Hayashi *et al.*, SN-1, a novel leukemic cell line with t(11;16)(q23;p13): myeloid characteristics and resistance to retinoids and vitamin D3. *Cancer Res* **60**, 1139 (Feb 15, 2000).
8. N. Niitsu, Y. Hayashi, Y. Honma, Downregulation of MLL-CBP fusion gene expression is associated with differentiation of SN-1 cells with t(11;16)(q23;p13). *Oncogene* **20**, 375 (Jan 18, 2001).

9. R. A. MacLeod, M. Voges, H. G. Drexler, Mono Mac 6: a mature monoblastic leukemia cell line with t(9;11)(p21;q23). *Blood* **82**, 3221 (Nov 15, 1993).

10. R. Gallagher *et al.*, Characterization of the continuous, differentiating myeloid cell line (HL-60) from a patient with acute promyelocytic leukemia. *Blood* **54**, 713 (Sep, 1979).

11. H. P. Koeffler, D. W. Golde, Human myeloid leukemia cell lines: a review. *Blood* **56**, 344 (Sep, 1980).

12. K. Mrozek, S. M. Tanner, K. Heinonen, C. D. Bloomfield, Molecular cytogenetic characterization of the KG-1 and KG-1a acute myeloid leukemia cell lines by use of spectral karyotyping and fluorescence in situ hybridization. *Genes Chromosomes Cancer* **38**, 249 (Nov, 2003).

Chapter 3

Family-wide Quantitative Interaction Maps for the Development of Bromodomain Inhibitors

Contributors: Katharin Shaw, Jun Qi, Michael McKeown, Xiang Xu, Alexander Federtion, William B. Smith, Roodolph St. Pierre Dennis Buckley, Minoru Tanaka, Stuart W. Ember, Ernst Schonbrunn, Matt Lindon, Jeremy P. Hunt, Lisa M Wodicka, Gabriel Pallares, Pietro Ciceri, Mark Floyd, Adam D. Torrey, Daniel K. Treiber, James Bradner

Introduction

Chromatin contains important regulatory information for all DNA-based processes, including transcription, repair, and replication. Histone tails extruding from the nucleosome core are subject to multiple modifications including phosphorylation, acetylation, methylation, ubiquitination and sumoylation. These modifications regulate transcription by modulating higher-order chromatin structures. Pharmacological control of transcription is receiving a resurgence of interest due to the recognition that dysregulation of transcription is a fundamental driver in numerous diseases including cancer and inflammatory disease. After the successful drugging of transcription through nuclear hormone receptors, there was a general perception that targeting general transcription factors would lead to pleiotropic and non-therapeutically useful effects. Further discouraging the development of transcription-targeting therapeutics was the impression that transcription factors and protein-protein interactions were "undruggable." Now, it is widely recognized that there are an abundance of posttranslational regulatory marks and corresponding enzymes that are druggable targets capable of modulating transcription; moreover, this modulation can have very specific effects due to the underlying transcriptional wiring in different cell types (*1*).

Two types of enzymes are responsible for these modifications— epigenetic writers that place marks on histones and other transcription factors and epigenetic erasers that remove these marks. Recognition of these marks by epigenetic reader proteins is an essential step in these regulatory processes. One class of epigenetic readers that has received considerable attention over the past several years are the bromodomain 'reader' proteins that recognize acetylated lysine residues. There are

sixty-one distinct human bromodomains that have been categorized into eight subfamilies based on primary, secondary, and tertiary structures (*2*) Recently developed small molecule inhibitors of BRD4, a member of the bromodomain extra-terminal domain (BET) subfamily have validated bromodomain inhibition as a viable therapeutic strategy (*2-4*). Chemical probes for BRD4 have demonstrated that BET bromodomain inhibition is a promising approach to treat a number of human diseases, such as cancer, inflammation, and heart failure. Currently, multiple BET inhibitors are being tested in human clinical trials (*5-8*).

Despite progress identifying drug-like BET inhibitors, there are relatively few small molecule inhibitors for non-BET bromodomains (*4, 9*), which has hindered the broad pharmacological interrogation of the bromodomain family. The discovery of small molecule inhibitors for diverse bromodomains has been limited in part by the absence of a broad, quantitative, and high-throughput biochemical assay platform to evaluate the potency and selectivity of small molecule collections across the bromodomain family. Current methods used to evaluate small molecule-bromodomain interactions include AlphaScreen (AS), Isothermal Titration Calorimetry (ITC), Differential Scanning Fluorimetry (DSF), and Surface Plasmon Resonance (SPR)— each of which has particular strengths but also limitations that preclude the high-throughput measurement of broad quantitative affinity and selectivity data. SPR and ITC are ideal for the measurement of thermodynamic K_D values but require large amounts of purified protein and are low throughput, interrogating only one family member at a time. AS is high-throughput, but is difficult to implement in a comprehensive panel format and reports IC_{50} values as opposed to true thermodynamic K_Ds. In contrast, DSF assesses

selectivity in higher throughput, but the measured ΔT_m data are semi-quantitative and most appropriate for defining relative potency. Here we report an assay platform (BROMO*scan*) that combines the quantitative features of SPR and ITC with the throughput of AS and the breadth of DSF. And we apply BROMO*scan* to rapidly discover and characterize novel bromodomain inhibitors with unprecedented selectivity profiles, to define selectivity for known bromodomain inhibitors and dual kinase-bromodomain inhibitors as well as to discover and characterize a novel dual LRRK2 kinase-bromodomain inhibitor.

Results

The BROMOscan assay platform and panel

BROMO*scan* expands upon our well-established KINOME*scan* kinase screening platform, which has enabled the evaluation of inhibitor potency and selectivity across more than 80 percent of the human kinome (*10-12*). KINOME*scan*, unlike traditional kinase enzyme activity assays, is a competitive inhibitor binding platform that does not measure enzyme activity, suggesting that the underlying principles should apply to non-enzyme drug targets, including bromodomains. We thus applied this platform to develop a comprehensive panel of bromodomain ligand binding assays. The panel includes twenty-four unique bromodomains (40% coverage of family) from seven subfamilies (*13*) (Figure 3.1A), with only subfamily VI (containing two members) not represented. The BET subfamily (II) is fully represented; subfamilies III, IV, V, and VII are represented by multiple examples, and subfamilies I and VIII are each represented by one domain.

BROMO*scan* assays include three components: 1) a bromodomain displayed on the surface of T7 phage particles; 2) magnetic affinity beads loaded with a known bromodomain-binding ligand (for example, a small molecule inhibitor or an acetylated peptide); 3) a test compound (or solvent control) (Figure 3.1B). In the absence of a test compound, the bromodomain interacts specifically with the affinity matrix and a significant number of phage particles is captured, and, after brief washing and elution steps, the number of phage particles captured is measured by qPCR of the phage genome. In the presence of a test compound that binds the targeted protein, the number of phage particles captured is reduced, resulting in a lower qPCR signal;

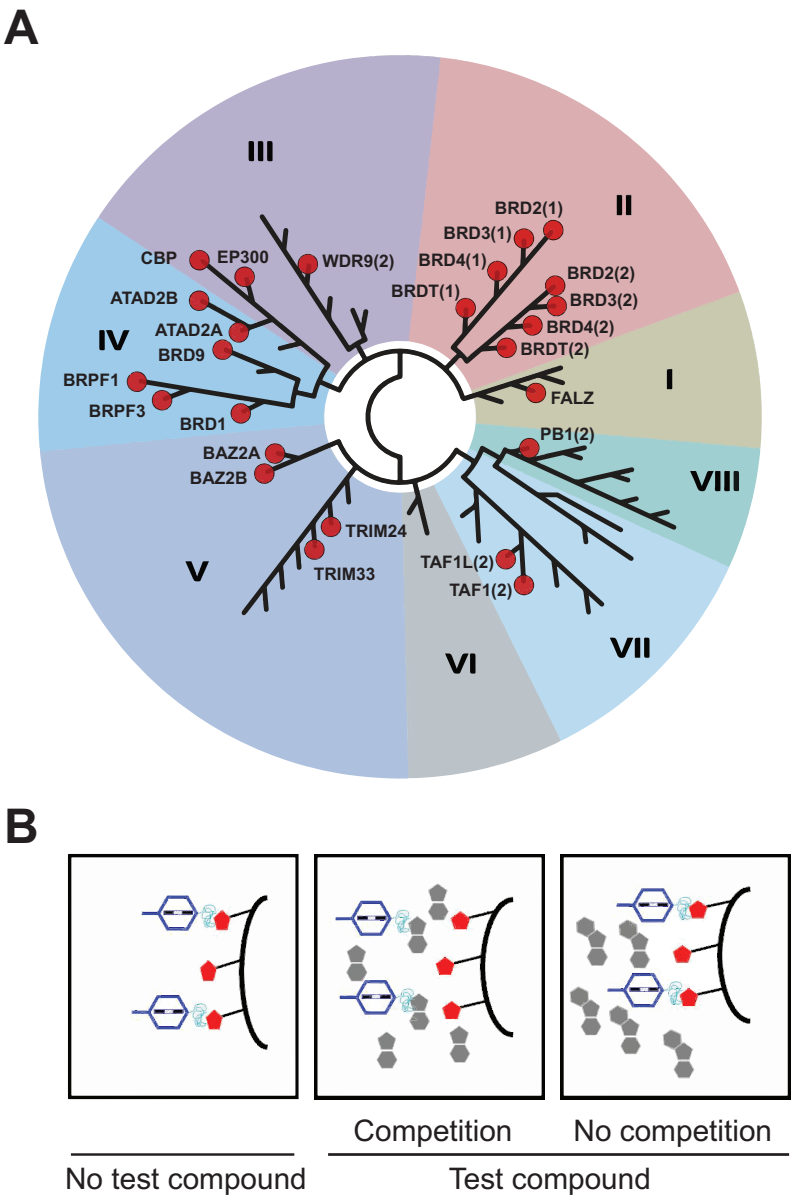

Figure 3.1 BROMO*scan* Panel and Schematic (A) The eight subfamilies of bromodomains,. Red markers indicate members represented in the BROMO*scan* panel **(B)** Schematic of BROMO*scan* assay

whereas for non-binding test compounds, the qPCR signal is unchanged relative to the solvent control. The assays are run at ultra-low (picomolar) protein concentrations, and the density of the capture ligands loaded on the magnetic affinity beads is carefully titrated to ensure the measurement of true thermodynamic binding constant (K_D) values for test compounds that are independent of the protein-capture ligand interaction affinity, as described (*14*). The bromodomain constructs and capture ligands used to build this assay panel are listed in Tables S3.1 and S3.2, respectively.

BROMOscan assay validation

We executed a multi-pronged assay validation approach that included: 1) measuring small molecule K_D values; 2) demonstrating selectivity for an acetylated histone peptide over its unmodified counterpart; and 3) measuring binding affinities for the acetyllysine mimetic solvent N-Methyl-2-pyrrolidone (NMP) (Figure S3.1A). Measured ligand affinities and selectivities were compared to published benchmarks when available. Unlike the case for kinase assay validation, there are relatively few known bromodomain ligands, and a significant fraction of the data are novel interactions discovered herein.

The BET assays were validated by testing the well-studied BET subfamily-selective inhibitor JQ1 (*13*) (Figure 3.2A). JQ1 has a stereogenic center, and the JQ1-S enantiomer is considerably more active than its enantiomer JQ1-R (*13*). Indeed, the K_D values of JQ1 via BROMO*scan* against the N- and C-terminal BRD4 bromodomains (BRD4(1) and BRD4(2), respectively) showed a strong preference for S-enantiomer

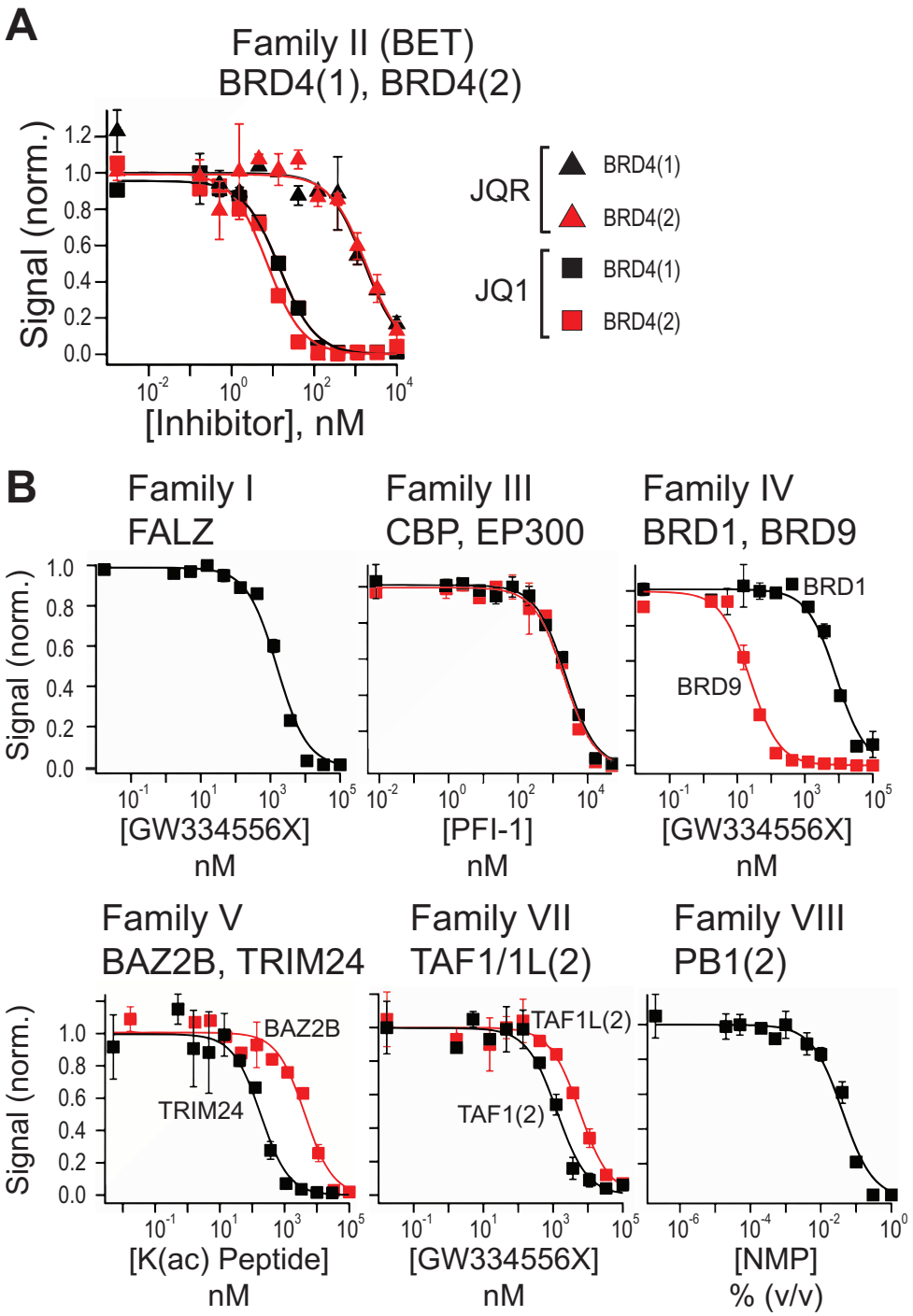

Figure 3.2 BROMO*scan* Assay Validation (A) Validation of Family II (BET) bromodomains using literature-reported JQ1 and its less active enantiomer JQ1-R against BRD4 site 1 and site 2 **(B)** Validation of non-BET bromodomains using literature-reported cross-reactive inhibitors or fragments, acetyled peptide ligands, and promiscuous solvent NMP

over R-enantiomer, and the data are in good agreement with published ITC and DSF data (*13*).

For the six subfamilies addressed outside of BET, dedicated small molecule inhibitors were limited when we initiated our assay development. Thus, assay validation was accomplished by testing cross-reactive BET inhibitors (for example PFI-1 (*15, 16*), a small published inhibitory fragment (GW334556X (*17*)), known or novel acetylated peptide ligands, and the promiscuous acetyllysine mimetic solvent NMP (*18*). Members of subfamilies I, IV, and VII were validated based on moderate- to high-affinity binding (nanomolar to low-micromolar) of GW334556X (Figure 3.2B). The subfamily III bromodomains CBP and EP300 bound with moderate affinity to PFI-1, consistent with an earlier report (*15*) and additional low affinity interactions measured for known inhibitors including JQ1 have literature precedent as well (*13*). Subfamily V members TRIM24 and BAZ2B bound to previously reported acetylated histone peptides with affinities consistent with literature values (Figure S3.1B, C) (*2*). In contrast, BAZ2B does not bind the corresponding non-acetylated peptide, while TRIM24 (containing only a PHD domain and bromodomain) lacks measureable affinity for a related truncated and methylated control peptide known to not interact with the PHD- or bromodomains (*19, 20*). The subfamily VIII bromodomain PB1(2) is generally refractory to inhibitor binding but nevertheless shows potent NMP binding (K_D = 0.05% v/v) and also has low but detectable GW334556X affinity (K_D = 140 mM).

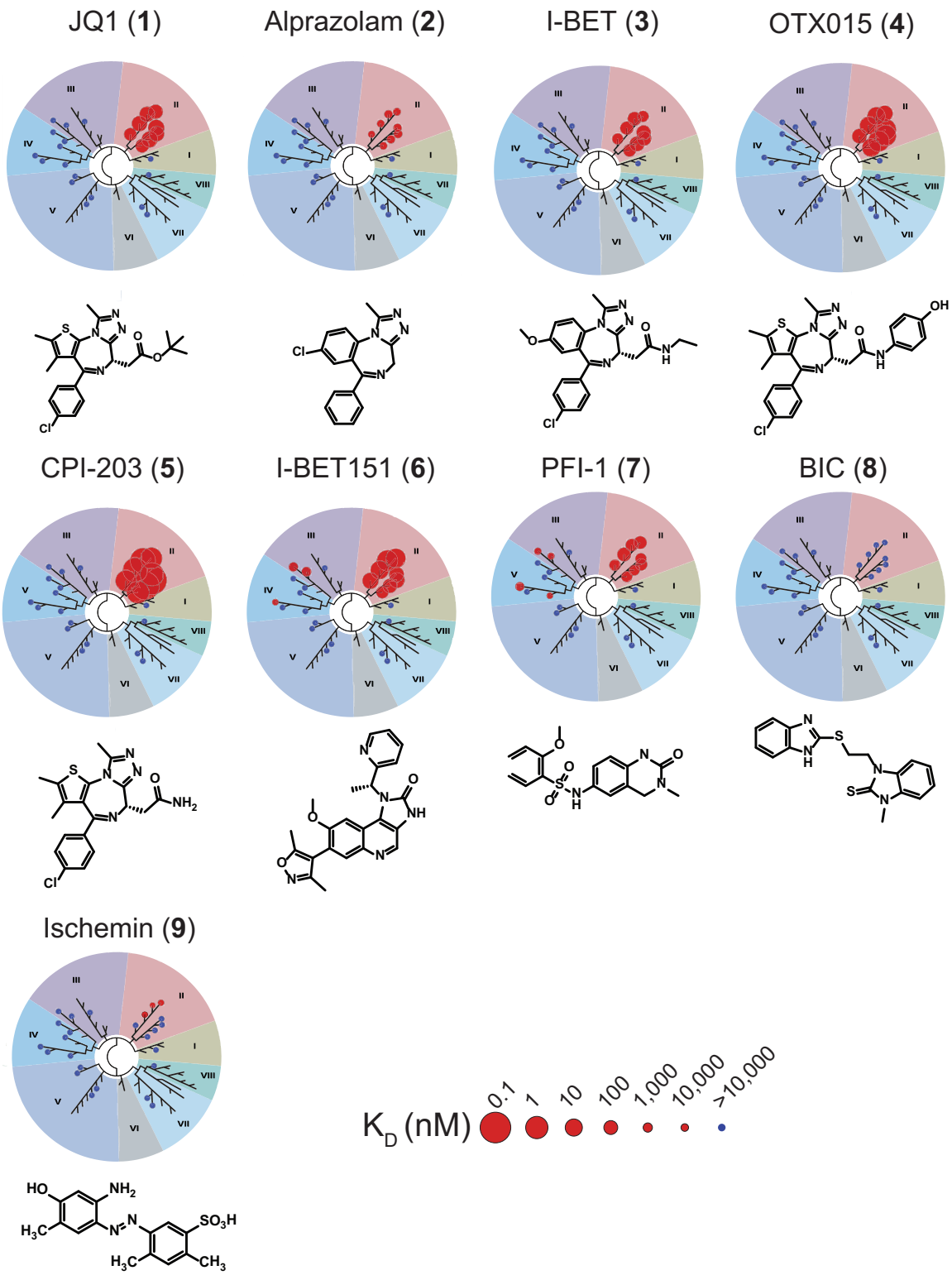

Figure 3.3 BROMO*scan* Interaction Maps for Literature-Reported Inhibitors Literature reported inhibitors profiled against the panel of bromodomains

Quantitative interaction maps for known bromodomain inhibitors

We generated interaction maps for several reported small molecule inhibitors by measuring K_D values across all 24 bromodomains (Figure 3.3). The thienodiazepine JQ1 (1), as anticipated, is remarkably BET-selective with low nanomolar activity across this subfamily and equal affinities for the N- and C- terminal bromodomains (domains (1) and (2), respectively). Additional benzodiazepine type BET inhibitors, including the FDA-approved benzodiazepine Alprazolam (2); and the thienodiazepine or benzodiazepine derivatives I-BET (3) (*21*), OTX-15 (4), and CPI-203 (5) (*22, 23*) exhibit selectivity profiles similar to JQ1, and exhibited agreement with literature-reported binding affinities. Compared to Alprazolam, the C6 position substituents for compounds 1 and 3-5 greatly increase potency of the thieno(benzo)diazepine core, which was suggested by co-crystal structures with BRD4 (*24*). These data confirm BET-selectivity for several widely used inhibitors across a broad and quantitative bromodomain assay panel.

We then evaluated known inhibitors with diverse binding motifs to further explore structure-activity relationships (SAR). IBET-151 (6), which binds through its 1,3-dimethylisoxazole ring, demonstrates potency and selectivity against the BET subfamily but, unlike the diazepines, also shows activity on subfamilies III (CBP,EP300) and IV (BRPF1) – a selectivity pattern that is largely recapitulated by the structurally distinct inhibitor PFI-1 (7). Two additionally known low-affinity inhibitors of BET bromodomains (BIC, (8)) or CBP (Ischemin, (9)) (*25*) showed little activity across the panel at the top concentration tested (10 micromolar). The BET inhibitor RVX-208 (10) (*26*) exhibits selectivity not only towards the BET subfamily but also for the second over the first

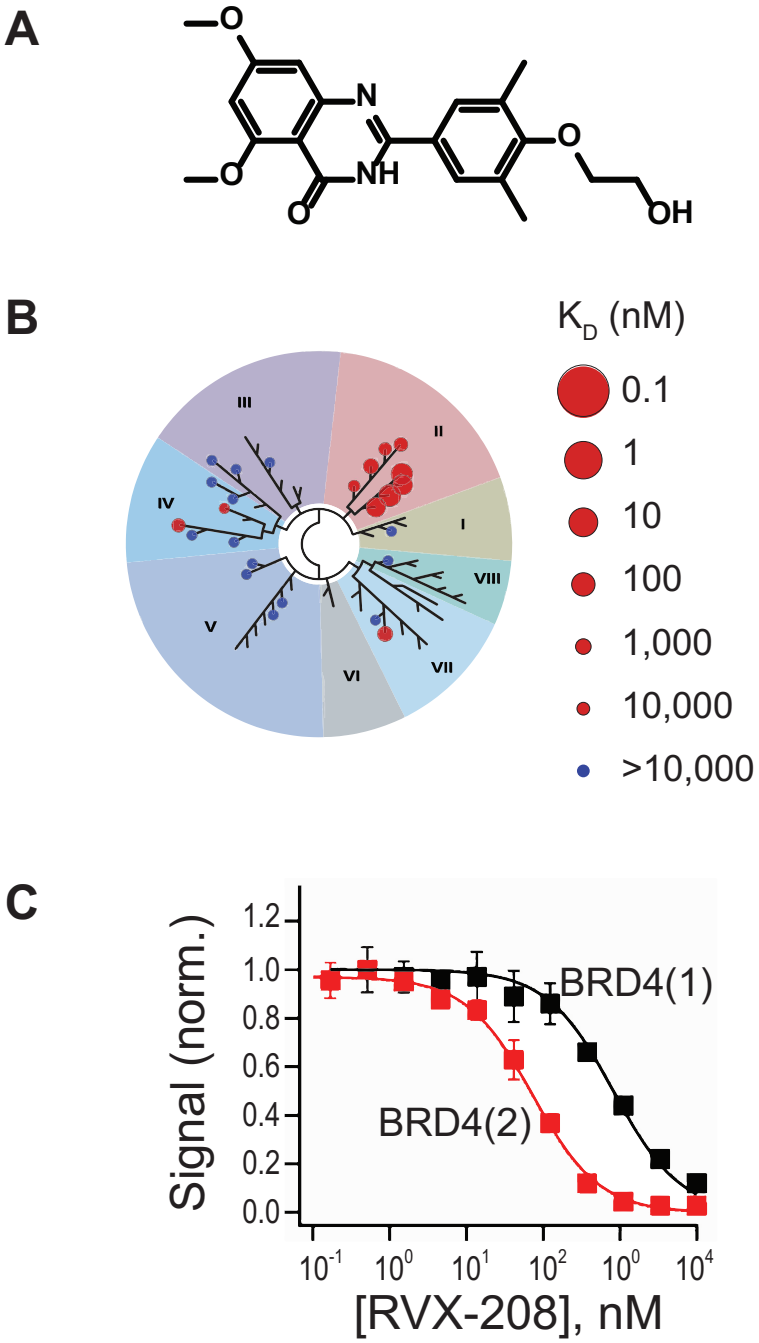

Figure 3.4 Selectivity Profiling for Compound RVX-208 (10) (A) Chemical structure of RVX-208 **(B)** Interaction map for RVX-208 **(C)** Inhibitory activity of RVX-208 against BRD4's first and second tandem bromodomains

tandem bromodomain in BET proteins (~10-fold preference), which is in agreement with published data (Figure 3.4) (*26*). Collectively, these data begin to identify scaffolds that have activity outside of the BET family, and the RVX-208 results further establish that BROMO*scan* assays detect moderate differences in binding affinity for closely related domains.

Discovery and evaluation of novel bromodomain inhibitors

BET inhibition has attracted significant attention in recent years, and the list of novel small molecule inhibitors reported in the scientific and patent literature continues to grow. We have evaluated a pyridilinone BET inhibitor, MT1 (11) (Figure 3.5A) recently described in the patent literature (*27-29*). As expected, MT1 exhibits potent and selective BET activity (Figure 3.5B), with CBP identified as the only off-target. Most interestingly, MT1 demonstrates a strong preference for the first tandem BET bromodomain over the second (~10-fold) (Figure 3.5C), which is a novel selectivity pattern – and a pattern opposite of that for RVX-208. Since asymmetric potency against these tandem BET domains can affect pharmacology and presumably toxicity as well, our demonstration that domain 1-selective BET inhibitors are possible reveals opportunities for next generation inhibitor design.

We solved a co-crystal structure of MT1 with BRD4(1) to define its binding mode. The lactam carbonyl group on the pyridilinone ring is the acetyllysine mimetic, interacting with the conserved Asn140 residue (Figure 3.5D and Figure S3.2A). The MT1 lactam functions similarly as the acetyllysine mimetics in JQ1 (triazole ring) and IBET-151 (1,3-dimethylisoxazole ring). These results define yet another important BET

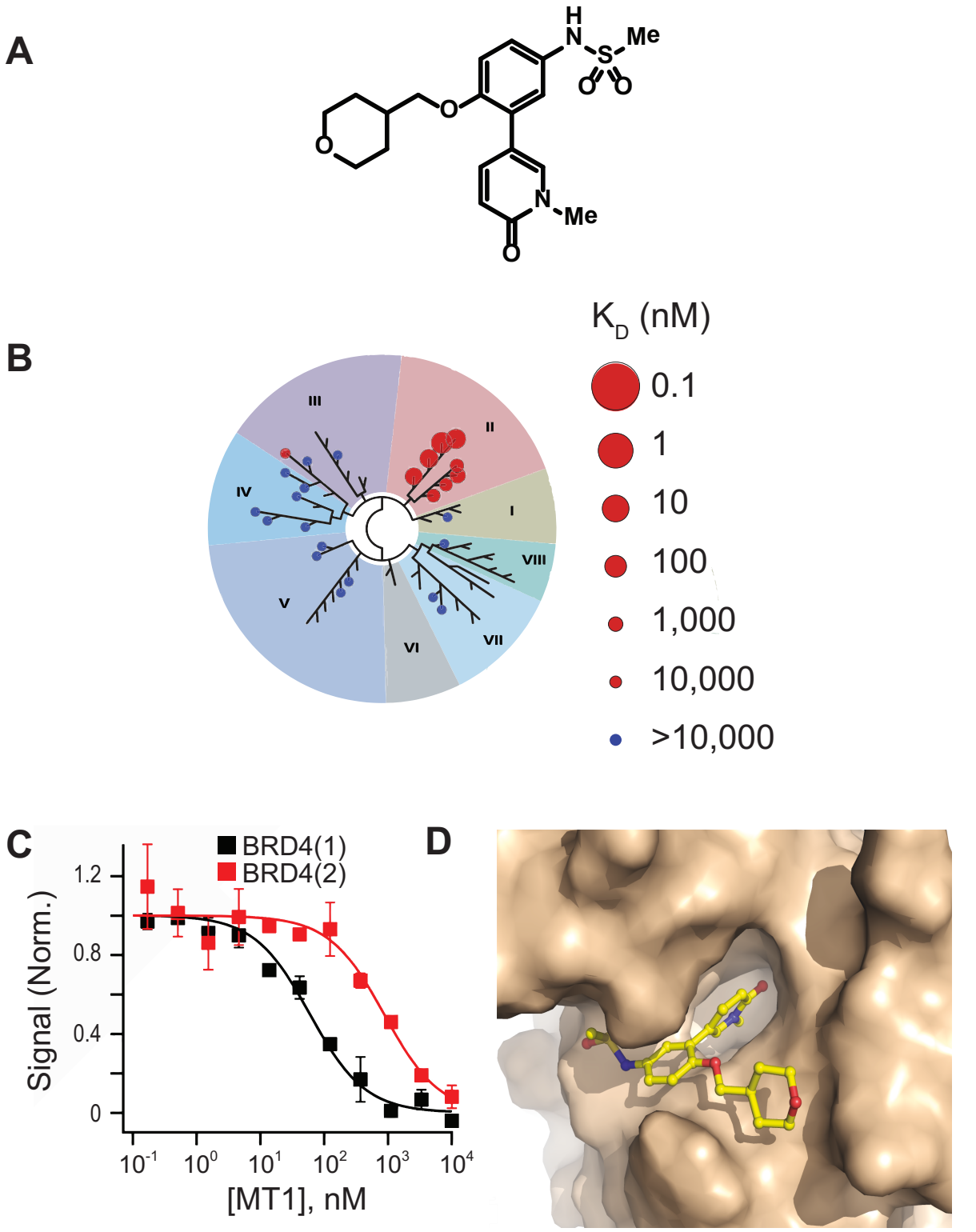

Figure 3.5 Selectivity Profiling for Compound MT1 (11) (A) Chemical structure of MT1 **(B)** Interaction map for MT1 **(C)** Inhibitory activity of RVX-208 against BRD4's first and second tandem bromodomains **(D)** Co-crystal of MT1 and BRD4(1)

family inhibitor binding mode but do not explain the tandem domain selectivity— a question that has been difficult to answer for RVX-208 as well (*26*).

We next used BROMO*scan* to guide and evaluate internal medicinal chemistry efforts focused on developing potent and selective inhibitors for non-BET bromodomains, and we describe the discovery of potent and selective CBP and BRD9 inhibitors. CBP contains a subfamily III bromodomain that has similarities to BET bromodomains and has potential roles in cancer (*30*). We initially developed parallel AlphaScreen assays for CBP, using a His_6-tagged CBP bromodomain paired with a biotinylated acetylated peptide, and BRD4(1), pairing His6-tagged protein with biotinylated JQ1 (*31*) (Figure S3.2B). This assay pair enabled us to screen for potent CBP inhibitors selective over BRD4(1). From a screen of >2,000 compounds we identified compound 20 (Figure S3.2C) as equally potent hit on CBP and BRD4(1). We further optimized this scaffold 12 for selective CBP inhibition by establishing SAR (Figure 3.6A), and installing a side chain at position R4 on the core further improved CBP-selectivity. The resultant optimized compound KS2222 (13) (Figure 3.6B) is 10-fold selective against CBP over BRD4(1) in AlphaScreen assays (Figure 3.6D). KS2222 was then evaluated by the BROMO*scan*, which confirmed selectivity for CBP over BRD4(1) and also revealed a high degree of unanticipated promiscuity across the bromodomain family, with TAF1(2) and TAF1L(2) (subfamily VII) as high affinity off-targets (Figure 3.6C). To further understand this novel selectivity profile, we modeled KS2222 by computational docking the compound into CBP and BRD4(1) crystal structures (Figure S3.3A, B). The CBP bromodomain binding pocket is narrower than the BRD4(1) pocket, and the small triazolophthalazine core unit enables KS2222 to be

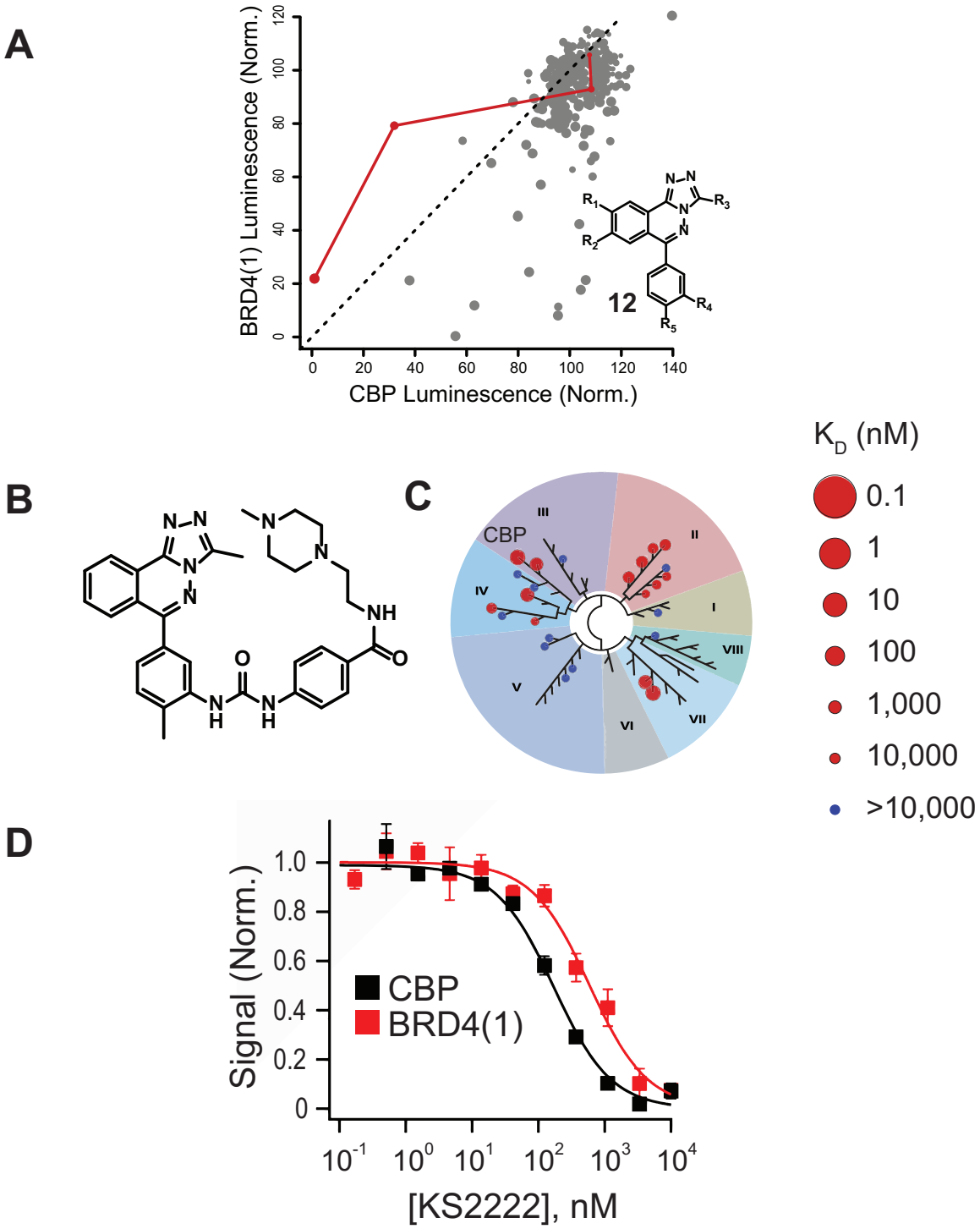

Figure 3.6 Selectivity Profiling for Compound KS2222 (13) (A) AlphaScreen assay screening library of compound similar to 12 **(B)** Chemical structure of KS2222 **(C)** Interaction map for KS2222 **(D)** KS2222 selectivity for CBP over BRD4(1)

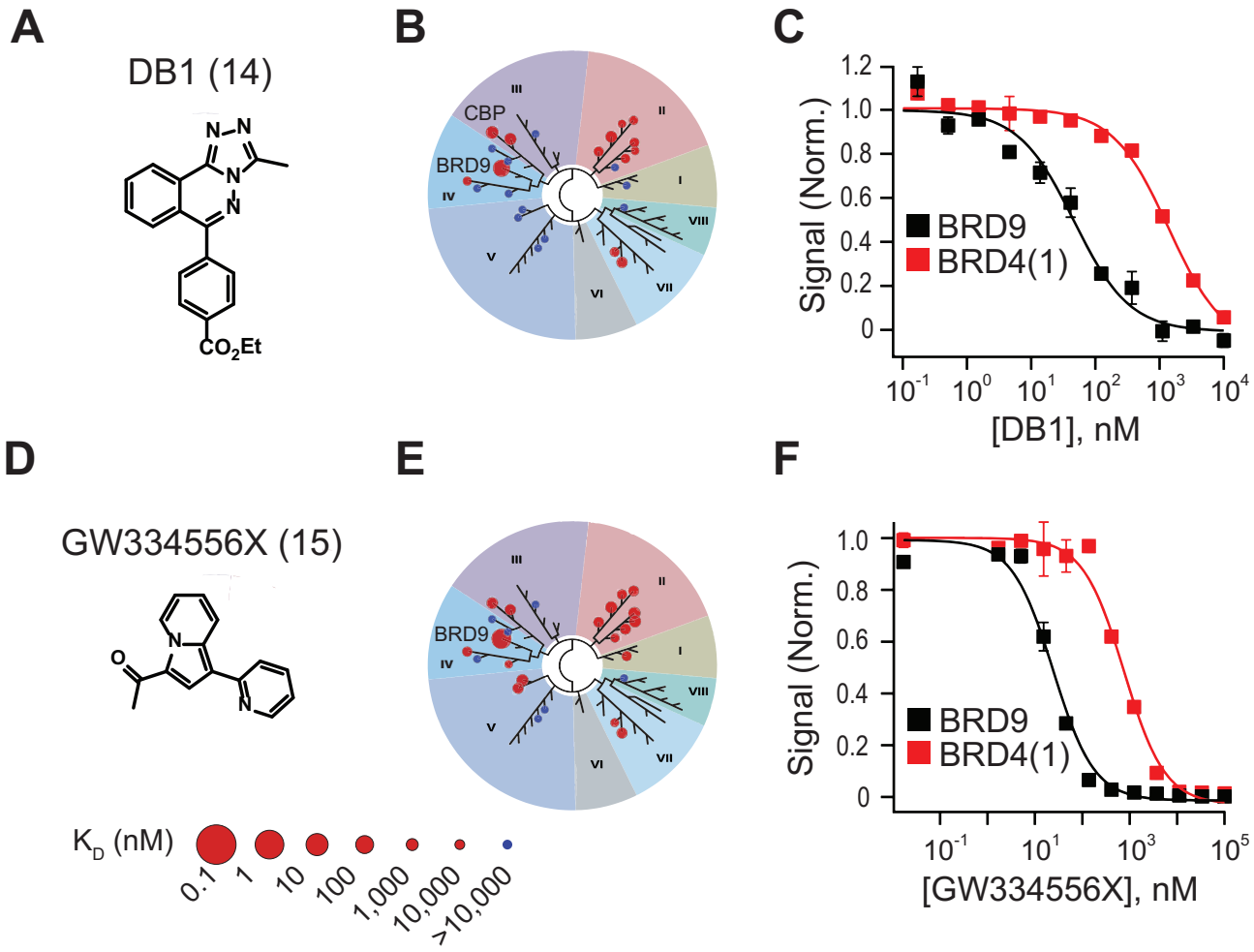

Figure 3.7 Selectivity Profiling for Novel Bromodomain Inhibitors (A) Chemical structure of DB1 (14) **(B)** Interaction map for DB1 **(C)** DB1 Selectivity for BRD9 over BRD4(1) **(D)** Chemical structure of GW334556X (15) **(E)** Interaction map for GW334556X **(F)** GW334556X selectivity for BRD9 over BRD4(1)

accommodated by both CBP and BRD4(1), but the phenyl side chain at position R4 interacts with CBP Arg1173 and Arg1169 through its carbonyl and piperazine ring, respectively, which improves selectivity over BRD4(1) compared to the original hit.

The relative promiscuity of KS2222 suggested that scaffold 12 may be a good starting point for discovering potent and selective inhibitors for diverse bromodomains. We thus generated BROMO*scan* interaction maps for multiple compound 12 derivatives. One such derivative with an R5 modification, DB1 (14) (Figure 3.7A, B), has excellent BRD9 potency (low nanomolar) and selectivity over BRD4(1) (30-fold) (Figure 3.7C). In addition, DB1, like KS2222, exhibits moderate to potent activity across four of the seven subfamilies addressed herein. Thus, we have identified scaffold 12 as a flexible starting point for the optimization of inhibitors for diverse bromodomains and demonstrate how the broad BROMO*scan* platform approach catalyzes discovery of novel chemical matter.

The small fragment GW334556X (15) was first described as a moderately potent BET inhibitor (Figure 3.7D) (*17*). During the course of several internal studies, including BROMO*scan* assay validation, we measured potent GW334556X activity on several diverse bromodomains, suggesting that this fragment is a promiscuous scaffold for novel inhibitor discovery. Indeed, the BROMO*scan* interaction map shows that GW334556X has the broadest activity of all compounds profiled herein – with potent to moderate activity against bromodomains from six of the seven subfamilies addressed (Figure 3.7E, F). GW334556X demonstrates moderate BET activity (high nanomolar to low micromolar) as expected, but its primary target is BRD9 (K_D = 24 nM); and despite this inhibitor's overall promiscuity, its relative BRD9 affinity is outstanding, with a 30-fold

selectivity over the next most potently inhibited target (BRD2(2)). To help rationalize GW334556X's selectivity profile, we developed a binding model based on the BRD9 crystal structure (Figure S3.3C). In this model, the small molecule ketone motif is the acetyllysine mimetic, interacting with Asn100 in the binding pocket. BRD9 has a more narrow binding pocket than BRD4(1), which enables GW334556X to interact with BRD9 Tyr106 via π stacking deep in the binding site and may explain its BRD9 selectivity. These results show that small bromodomain inhibitory fragments can have remarkable ligand efficiencies as well as the potential to be optimized for the inhibition of diverse bromodomains.

Identification and characterization of dual kinase-bromodomain inhibitors

It was recently shown that several well-studied kinase inhibitors potently cross-react with BET bromodomains (*32-34*). We thus initiated a dual kinase-bromodomain inhibitor discovery campaign with the goals of: 1) identifying additional cross-reactive kinase inhibitors; 2) using BROMO*scan* to define quantitative bromodomain interaction maps for both known and novel cross-reactive kinase inhibitors; 3) applying structural methods to define novel binding modes. To achieve the first goal, we evaluated: 1) a large panel of known kinase inhibitors (LINCS panel) (*35*) using the BRD4(1) AS assay; and 2) a previously described mature inhibitor set (*11*) using our BRD4(1) AS assay (Figure 3.8A, S3.4A). These screens identified several previously described (*32, 33*) diverse cross-reactive kinase-inhibitors, including the related PLK inhibitors BI-2536 and BI-6727/volasertib (18); the JAK2 inhibitor TG-101348; the related p38 inhibitors SB-202190 (16) and SB-203590 (17) (Figure 3.8B); and the PI3K/mTOR inhibitor PP242.

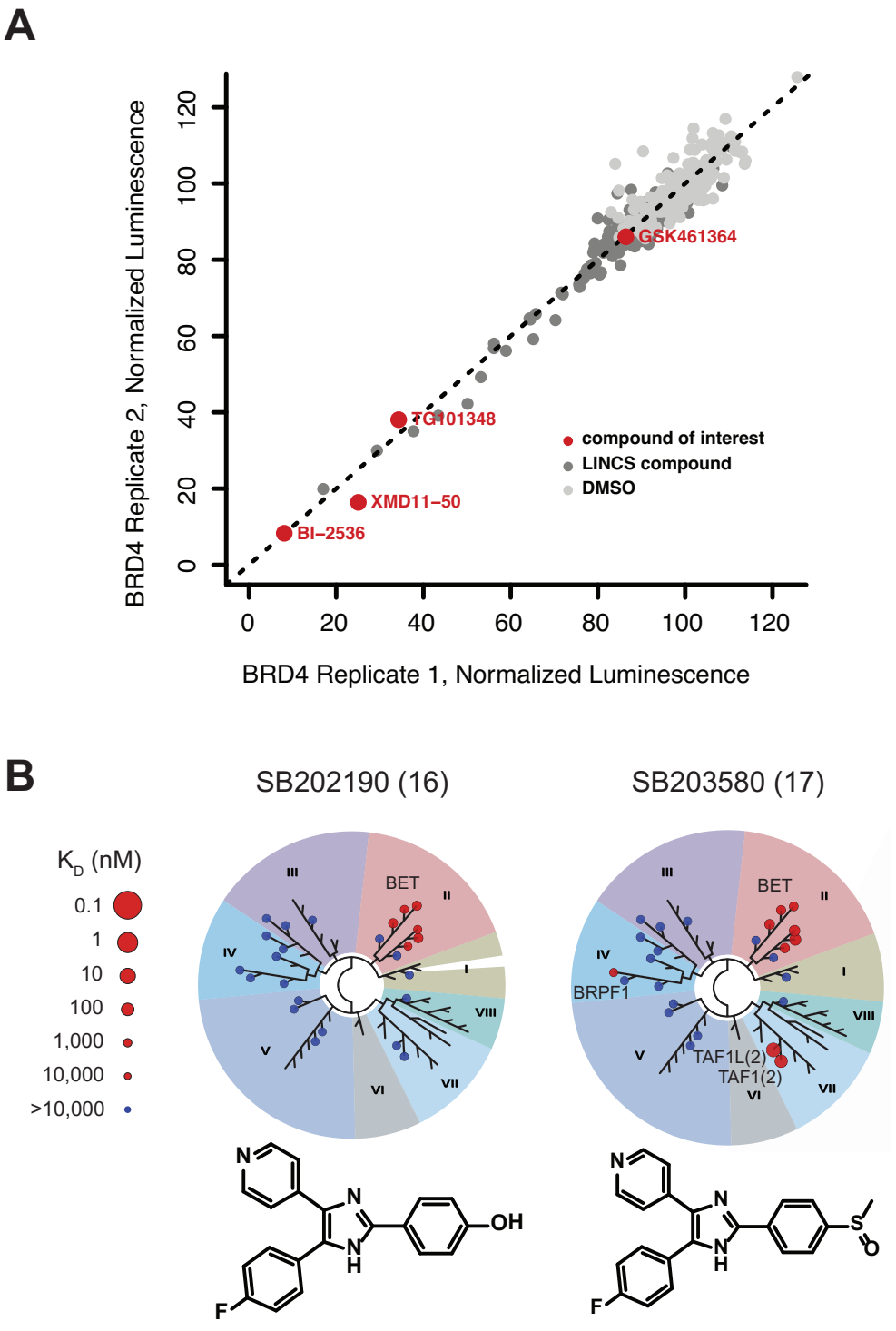

Figure 3.8 Identification and Characterization of Dual Kinase-Bromodomain Inhibitors (A) BRD4(1) AlphaScreen against LINCS panel of compounds **(B)** Interaction maps for p38 kinase inhibitors

Most interestingly, the LINCS panel screen identified the selective LRRK2 kinase inhibitor XMD11-50 (19) (*36*) as a novel potent dual kinase-BRD4(1) inhibitor, and this result is of significance since LRRK2 has been identified as a potential Parkinson's Disease target (*37*), and XMD11-50 (19) is used pharmacologic probe compound for this indication.

BROMO*scan* interaction maps for all identified dual kinase-bromodomain inhibitors show BET-selective patterns but also interactions with diverse bromodomains from multiple additional subfamilies. In particular, the two closely related p38 inhibitors SB-202190 (16) and SB-203590 (17), which have identical kinome-wide inhibitory profiles (*32*), nevertheless show distinct interaction maps, where, remarkably, the subtle change from a hydroxyl in (16) to a sulfoxide in (17) confers potent TAF1(2) and TAF1L(2) activity (high nanomolar) (Figure 3.8B). Although the bromodomain interaction maps for previously reported dual inhibitors are similar to those measured in an earlier study using DSF (*32*), the more sensitive BROMO*scan* method detects important additional interactions with TAF bromodomains that enable further SAR analysis. These data establish that it is possible to design dual kinase-bromodomain inhibitors with identical kinome-wide inhibitory profiles but different bromodomain inhibitory profiles— a finding complementary to the previous observation that it is possible to maintain a bromodomain inhibitory profile while changing the kinase selectivity (*32*).

The PLK inhibitors and the LRRK2 inhibitor XMD11-50 (19) are particularly potent on the BET family, with double-digit nanomolar affinity in BROMO*scan* and potent activity in ITC (Figure 3.9A, B, 3.10A, B) as well, whereas the other inhibitors

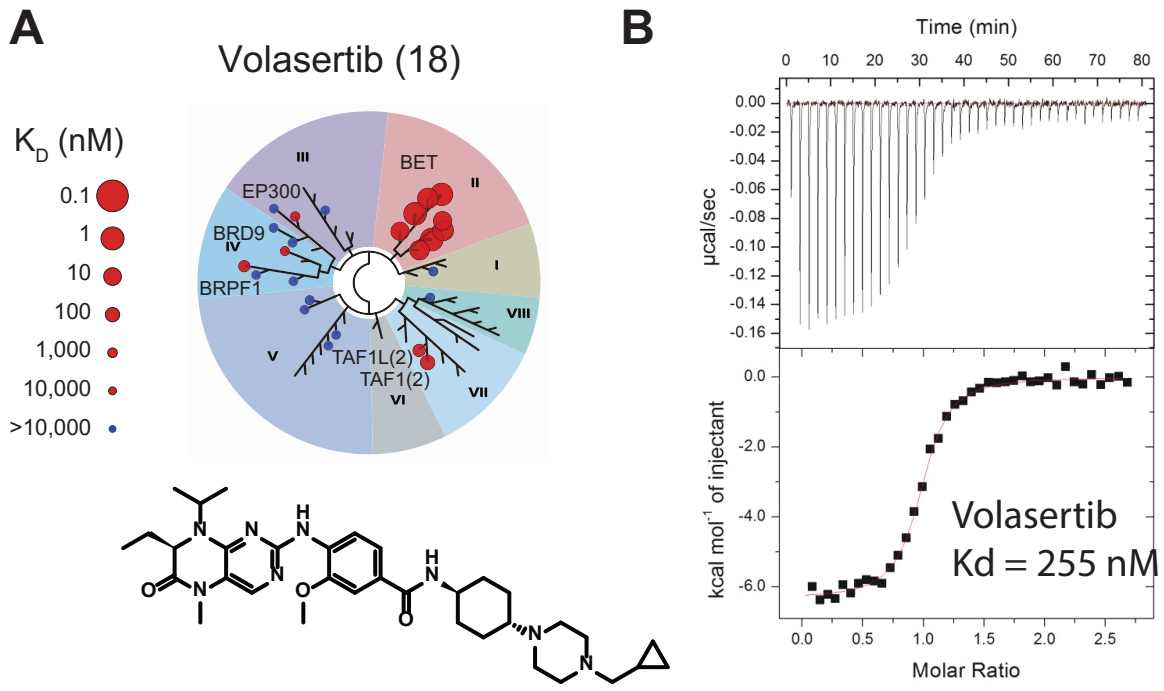

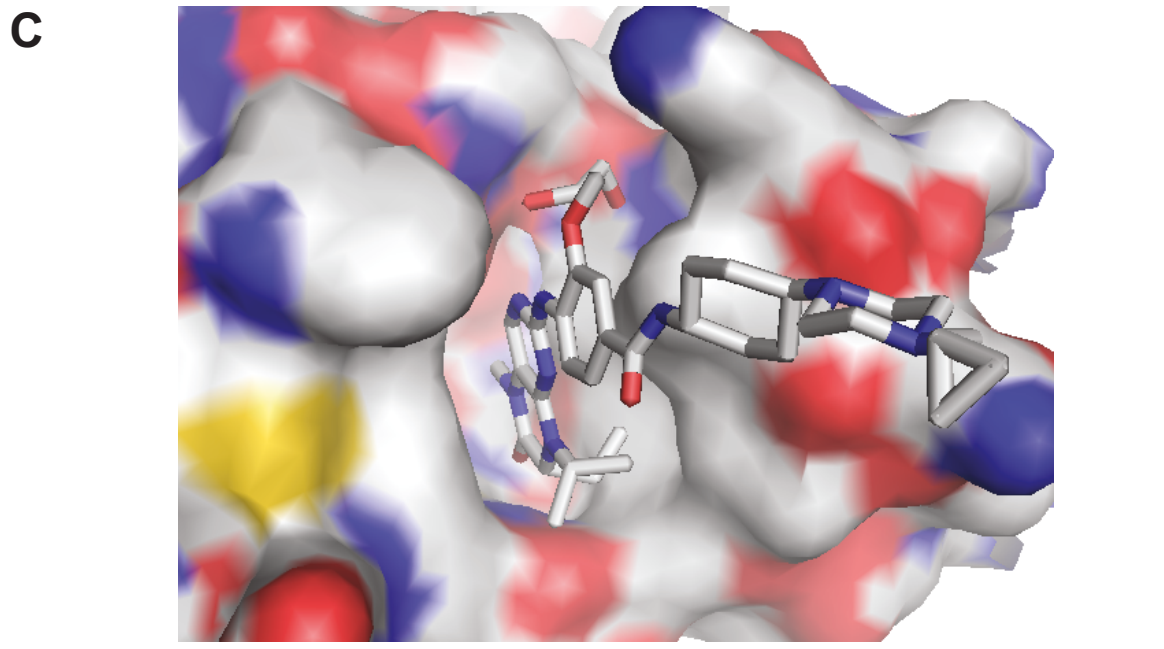

Figure 3.9 Identification and Characterization of Volasertib (A) Interaction map of Volasertib **(B)** ITC with BRD4(1) and Volasertib **(C)** Co-crystal of BRD4(1) and Volasertib

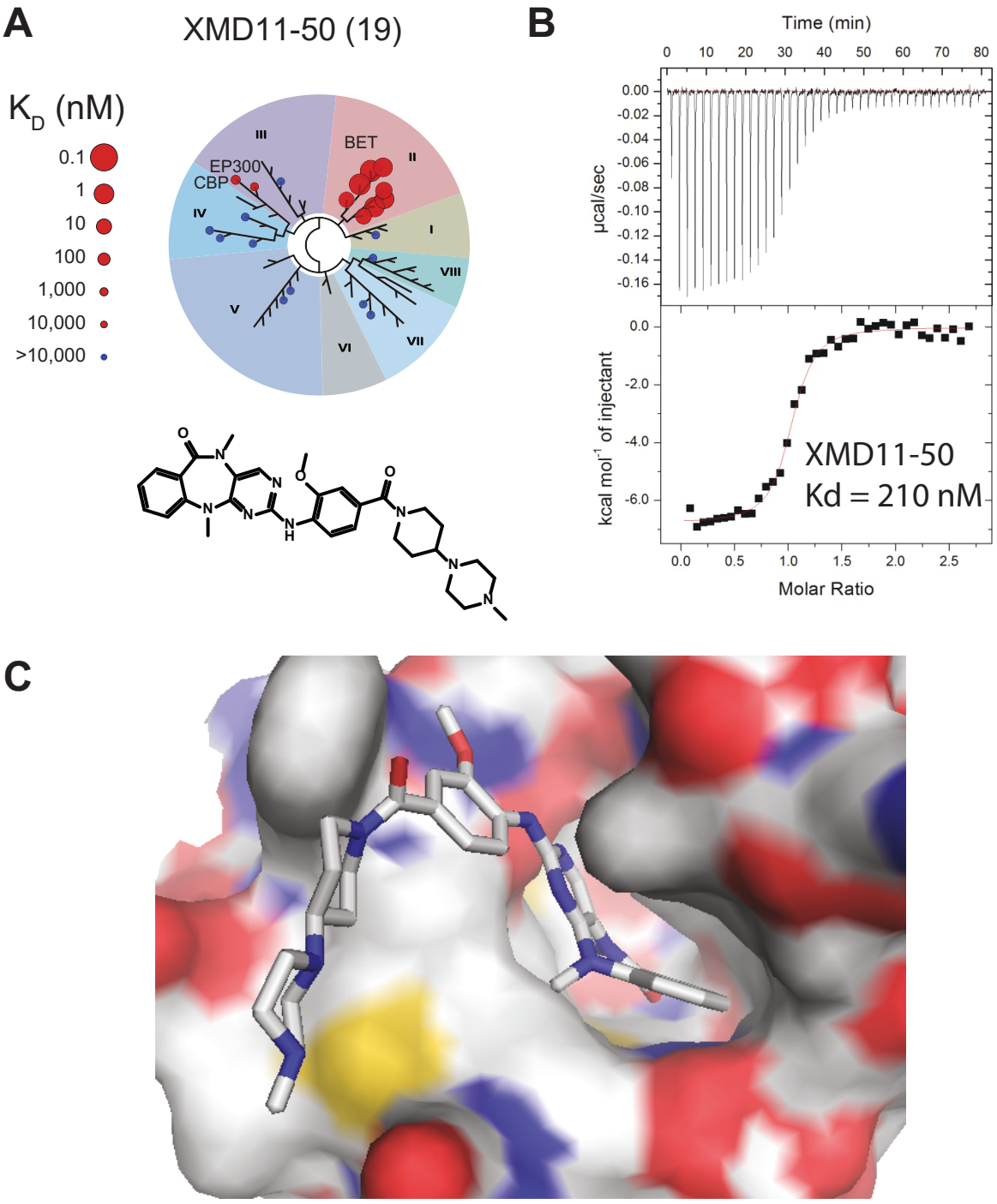

Figure 3.10 Identification and Characterization of XMD11-50 (A) Interaction map of XMD11-50 **(B)** ITC with BRD4(1) and XMD11-50 **(C)** Co-crystal of BRD4(1) and XMD11-50

have low micromolar BET activity. We next solved BRD4(1) co-crystal structures for the clinically advanced PLK inhibitor BI-6727/volasertib (18) and the LRRK2 inhibitor XMD11-50 (19) to define the binding modes and to predict how these scaffolds further direct the medicinal chemistry effort around modifying the dual kinase-bromodomain inhibitory activity against either kinases or bromodomains. The BI-6727/volasertib (18) lactam ring carbonyl interacts with conserved Asn140, which, together with high shape complementarity, provide strong BET affinity and likely explain the moderate activities on non-BET bromodomains as well (Figure 3.9C, S3.4B). The XMD11-50 (19) co-crystal structure shows how the novel and much larger ring system is also accommodated by the binding pocket and that the amide in the seven member ring interacts with Asn140 (Figure 3.10C, S3.4C). The binding affinity is likely enhanced by π-stacking between Trp81 and the inhibitor's phenyl ring. Despite XMD11-50 (19)'s large binding motif, it nevertheless retains moderate CBP activity and could be a valuable scaffold for developing selective inhibitors for this target.

Cellular activity of dual kinase-bromodomain inhibitors

To confirm that XMD11-50 (19) and BI-6727/volasertib (18) engage BRD4(1) in a cellular milieu, we employed InCELL Hunter™ assays, which monitor ligand binding-induced protein stabilization in human cells (*38*). Both BI-6727/volasertib (18) and XMD11-50 (19) show activities similar to the positive controls JQ1 (1) and its close derivative BI-2536, whereas control LRRK2 and PLK inhibitors lacking bromodomain affinity, NVP-TAE-684 and GSK-451364A, respectively, are inactive (Figure 3.11A).

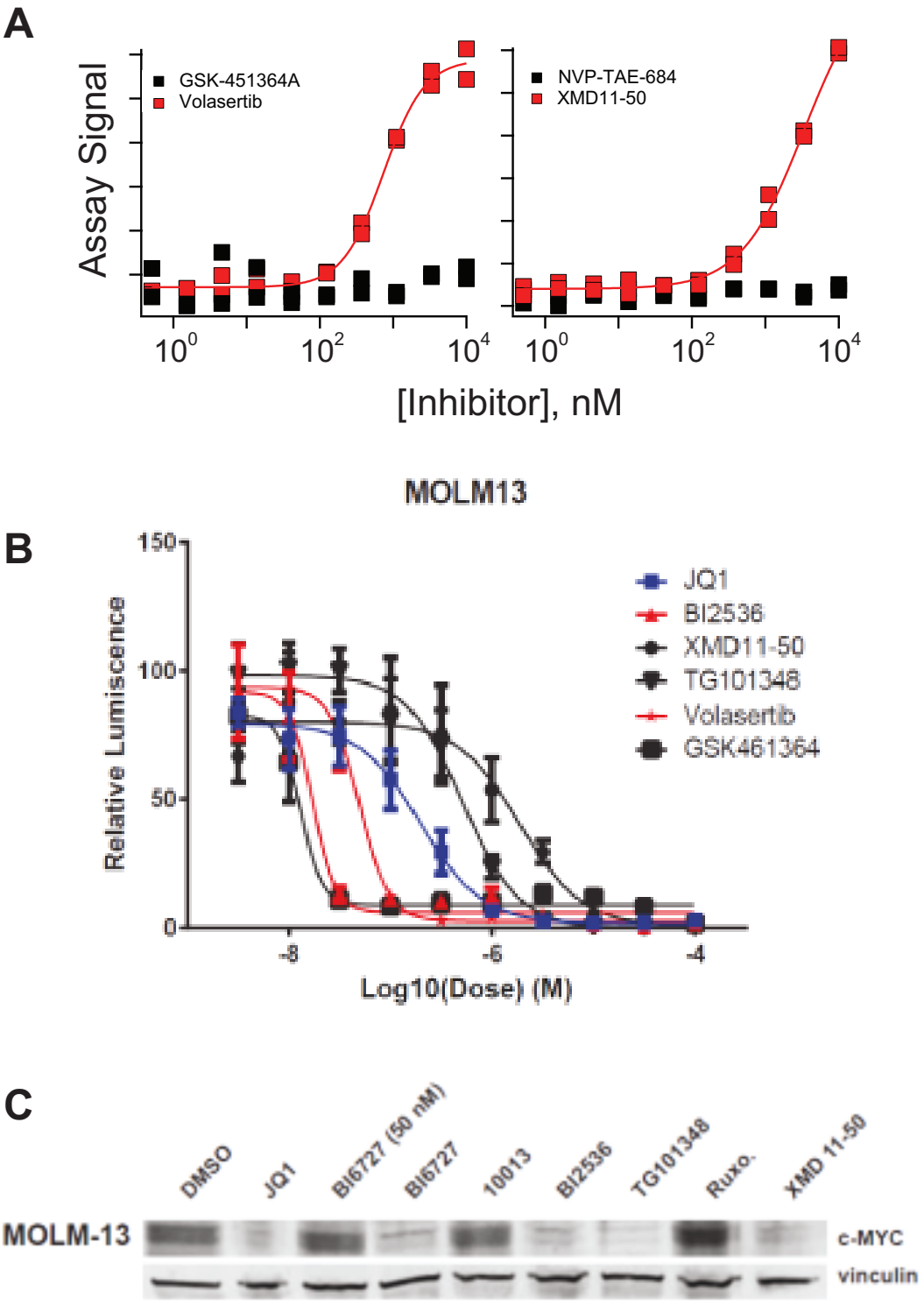

Figure 3.11 Cellular Activity of Dual Kinase-Bromodomain Inhibitors **(A)** Cellular target engagement of BRD4(1) by InCELL Hunter™ assays **(B)** Cellular viability of MOLM13 cells treated with inhibitors **(C)** Western blot against c-MYC in MOLM13 cells treated with inhibitors

Collectively, these data confirm potent cellular BRD4(1) engagement for XMD11-50 (19) and BI-6727/volasertib (18).

In order to further define the cancer cell pharmacology of these dual kinase-bromodomain inhibitors, the small molecules were examined in both the BRD4-dependent midline carcinoma cell line 797 and in MOLM13, a leukemia cell line that is sensitive to bromodomain inhibition due to its exquisite Myc-dependence (*3, 39*). These kinase inhibitors exhibited a strong antiproliferation effect in both cell lines (Figure 3.11B, S3.5A). Because Myc down-regulation in the MOLM13 line is the signature of BRD4 bromodomain inhibition, we evaluated bromodomain inhibition of these molecules by determining cellular Myc levels after treatment (*3, 39*). At a 1 μM concentration, dual-function kinase inhibitors down-regulated Myc as expected, but kinase-only inhibitors did not (Figure 3.11C). Interestingly, compound 18 at a low concentration (50 nM) did not appreciably down-regulate Myc, as this concentration has not yet reach bromodomain inhibition level. These data indicate that dual kinase-bromodomain inhibitors distinguish themselves from kinase-only inhibitors, such as GSK461364 and Ruxolitinib, in their function within cancer cells. Cell cycle studies in BRD4-dependent cell line 797 demonstrated the unique behavior of dual-function molecules. Kinase-bromodomain inhibitors acted as bromodomain inhibitors— similarly to JQ1— at high concentrations, causing G1 arrest rather than the G2 arrest exhibited by kinase-only inhibitor treatment (Figure S3.5B).

Through these experiments, we have utilized BROMO*scan* to discover novel bromdomain activity of kinase inhibitors. The newly identified activity of kinase inhibitors can be used to further discover and develop bromodomain inhibitors with

different scaffolds. Moreover, evaluating the cellular functionality of these molecules is important for understanding dual-function inhibitors, and more importantly, it could potentially identify biomarkers for clinical study. This discovery further proved that the BROMO*scan* is a powerful tool to identify novel activity of known compounds. Overall, we have developed a set of phage display assays that can be utilized as a platform to assess the potency and selectivity of small molecule inhibitors against bromodomains. We have also demonstrated that we can use this assay platform to identify novel inhibitors and potentially facilitate the development of potent and selective bromodomain inhibitors.

Discussion

Our cognizance of the extent to which epigenetic readers are involved in disease pathology— from cancer to inflammation to heart failure— has been crucially facilitated by the discovery and development of small molecule inhibitors (such as JQ1) for BET bromodomains. Because of a dearth of small molecule inhibitors, the depth of our understanding does not extend beyond the BET subfamily of bromodomains. Development of potent and selective small molecule inhibitors has been hampered by the absence of a comprehensive assay platform— a large panel of assays capable of evaluating small molecule potency and selectivity across a close family of proteins. There are multiple challenges in creating such an assay platform, including purifying a variety of proteins at large-scale, accurately assessing thermodynamic binding across a protein family, and maintaining a broad dynamic range in order to both sensitively identify low-potency inhibitors and differentiate high-potency inhibitors.

To surmount these difficulties, we exploited phage display assay technology. Because most of the bromodomains are domains found within large multi-domain proteins— which are themselves part of much larger complexes— maintaining binding ability has made isolation of the bromodomain and subsequent purification difficult. Most biophysical characterization assays, such as SPR or ITC, require large quantities of protein. In using phage display, we eliminate arduous protein purification steps while maintaining the ability to accurately calculate thermodynamic binding over a broad dynamic range. The resulting BROMO*scan* platform has an attractive biochemical regime that confers significant advantages over other valuable assay formats such as AS, ITC, and DSF, including: 1) measurement of true thermodynamic K_D values as

opposed to relative IC_{50}s or DT_m in AS and DSF, respectively; and 2) a broad dynamic range for accurate K_D measurements (picomolar to millimolar) that avoids ITC's "tight binding limit" for interactions where the protein concentration is significantly higher than the test compound K_D. And because these phage display-based assays do not require painstaking protein purification steps, we have been able to extend our panel to include a large number and variety of bromodomains through rapid development and validation.

We have fully validated the BROMO*scan* platform using several reported bromodomain inhibitors and substrate peptides with potencies ranging from nanomolar to high micromolar. Data generated using other assay formats, namely DSF and AS, corroborated our BROMO*scan* data. Additionally, the K_D data generated by BROMO*scan* were in good agreement with literature reported K_D data determined using biophysical measurements such as ITC and SPR. Thus, we have demonstrated that we can comprehensively evaluate compound potency and selectivity in agreement with commonly used assays. We are aware that the bromodomain field is young, and published K_D values are limited. Further expansion the platform coverage and validation of these assays with growing field of small molecule bromodomain inhibitors will be important to establish the credibility of our assay panel.

After thorough validation, we demonstrated the BROMO*scan* platform's flexibility in addressing a variety of scientific problems. Using BROMOscan, we were able to discover the inhibitory activity of small molecules against novel bromodomains other than their reported targets. The assay platform also informed our medicinal chemistry effort in developing novel scaffold into potent, selective inhibitors for non-BET bromodomain family members such as CBP and BRD9. This could be further extended

to other family members such as TAF1 and TAF1L. BROMO*scan* also enabled our discovery of novel biochemical activity against bromodomains of small molecules initially developed for kinases. Knowledge of the dual-function nature of these inhibitors has furthered our understanding of drug mechanism in cancer. Through these experiments, we establish this assay platform as a powerful tool in chemical probe discovery and development and in clinical investigation through elucidating drug mechanisms in disease.

Overall, we have developed an assay platform that can be used to evaluate accurate binding affinity as well as comprehensive selectivity. The panel can be considered as excellent counter-profiling platform for other assay formats. The data generated by the assay are reliable with great reproducibility, and we foresee that our assay platform will facilitate small molecule inhibitor development for bromodomains as well as determine potential bromodomain activity of other non-obvious scaffolds. Evaluating the bromodomain activity of clinical compounds could also be useful in mechanism elucidation and discovering additional biomarkers of clinical compounds.

Methods

All the compounds used in this study have been either synthesized in Bradner Laboratory or Gray Laboratory at Dana-Farber Cancer Institute or directly purchased from commercial vendors. All the compound structures and batch purities (≥ 95%) has been confirmed by using standard analytical methods (HPLC/mass spectroscopy and NMR). The proteins used in this study (BRD4(1) and CBP) was purified by following the detail description in supporting information. The AlphaScreen assay development and condition can be found in detail as described in reported protocol (J Roberts, J Bradner, Current Protocol). Cell line 797 and MOLM13 were cultured were cultured at 37°C in 5% CO_2 and grown in RPMI (Cellgro), supplemented with 2 mM L-glutamine, 50 U/mL penicillin, 50 U/mL streptomycin and 10% fetal bovine serum (FBS, all from Invitrogen).

BROMOscan assays. T7 phage strains displaying bromodomains were grown using an E. coli host derived from the BL21 strain as described (*10*). Bromodomain constructs are listed in Table S3.1. Streptavidin-coated magnetic beads were treated with biotinylated small molecule or peptide ligands for 30 minutes at room temperature to generate affinity resins for bromodomain assays. Immobilized ligand – assay pairs are listed in Table S3.2. The experimental details were described in SI. All ligand loading densities were optimized for the measurement of true thermodynamic test compound K_Ds as described (*14*).

Acknowledgments

We acknowledge the KINOME*scan* screening and development team is for measuring inhibitor K_D values, P. Gallant and P. Khanna for helpful discussions and for critically reading the manuscript.

Author contributions

J.E.B., D.K.T., and J.Q. designed and developed the project. J.P.H. directed BROMO*scan* assay development and validation efforts, L.M.W., G.P., A.D.T, and C.E.A. built and validated BROMO*scan* assays and optimized assays for high throughput data collection, and P.C. and M.F. designed, cloned, and expressed all BROMO*scan* bromodomain constructs. M.J.L. provided GW334556X and made valuable intellectual contributions on how to use this reagent to build and to validate BROMO*scan* assays. J.Q., K.S. and J.E.B. designed and supervised the syntheses of novel and literature reported bromodomain inhibitors. M.R.M. and K.S. designed and developed AlphaScreen assays. A.J.F. and J.Q. conducted the computational modeling. X.X., S.W.E., and E.S. generated crystal and solved structure. K.S., W.S., and M.R.M. performed cellular studies. D.K.T and J.E.B directed the studies, and J.Q., K.S., J.E.B, and D.K.T. wrote the document.

Competing financial interests

D.K.T, P.C., A.D.T, J.P.H., L.M.W, M.F., and G.P. are employees of DiscoveRx Corporation. M.J.L is an employee of GlaxoSmithKline.

References

1. D. Filipescu, S. Muller, G. Almouzni, Histone H3 variants and their chaperones during development and disease: contributing to epigenetic control. *Annual review of cell and developmental biology* **30**, 615 (2014).
2. P. Filippakopoulos *et al.*, Histone recognition and large-scale structural analysis of the human bromodomain family. *Cell* **149**, 214 (Mar 30, 2012).
3. J. E. Delmore *et al.*, BET bromodomain inhibition as a therapeutic strategy to target c-Myc. *Cell* **146**, 904 (Sep 16, 2011).
4. A. Puissant *et al.*, Targeting MYCN in neuroblastoma by BET bromodomain inhibition. *Cancer discovery* **3**, 308 (Mar, 2013).
5. GlaxoSmithKline. Clinicaltrials.gov. "A Study to Investigate the Safety, Pharmacokinetics, Pharmacodynamics, and Clinical Activity of GSK525762 in Subjects With NUT Midline Carcinoma (NMC) and Other Cancers" (Bethesda (MD): National Library of Medicine (US), NLM Identifier: NCT01587703, 2012; https://clinicaltrials.gov/ct2/show/NCT01587703)
6. Oncoethix GmbH. Clinicaltrials.gov. "A Phase I, Dose-finding Study of the Bromodomain (Brd) Inhibitor OTX015/MK-8628 in Hematologic Malignancies (MK-8628-001)" (Bethesda (MD): National Library of Medicine (US), NLM Identifier: NCT01713582, 2012; https://clinicaltrials.gov/ct2/show/NCT01713582)
7. Constellation Pharmaceuticals. Clinicaltrials.gov. "A Phase 1 Study Evaluating CPI-0610 in Patients With Progressive Lymphoma" (Bethesda (MD): National Library of Medicine (US), NLM Identifier: NCT01949883, 2013; https://clinicaltrials.gov/ct2/show/NCT01949883)

8. Hoffmann-La Roche. Clinicaltrials.gov. "A Two Part, Multicenter, Open-label Study of TEN-010 Given Subcutaneously" (Bethesda (MD): National Library of Medicine (US), NLM Identifier: NCT01987362, 2013; https://clinicaltrials.gov/ct2/show/NCT01987362)

9. F. M. Ferguson *et al.*, Targeting low-druggability bromodomains: fragment based screening and inhibitor design against the BAZ2B bromodomain. *Journal of medicinal chemistry* **56**, 10183 (Dec 27, 2013).

10. M. A. Fabian *et al.*, A small molecule-kinase interaction map for clinical kinase inhibitors. *Nature biotechnology* **23**, 329 (Mar, 2005).

11. M. I. Davis *et al.*, Comprehensive analysis of kinase inhibitor selectivity. *Nature biotechnology* **29**, 1046 (Nov, 2011).

12. M. W. Karaman *et al.*, A quantitative analysis of kinase inhibitor selectivity. *Nature biotechnology* **26**, 127 (Jan, 2008).

13. P. Filippakopoulos *et al.*, Selective inhibition of BET bromodomains. *Nature* **468**, 1067 (Dec 23, 2010).

14. L. M. Wodicka *et al.*, Activation state-dependent binding of small molecule kinase inhibitors: structural insights from biochemistry. *Chemistry & biology* **17**, 1241 (Nov 24, 2010).

15. P. V. Fish *et al.*, Identification of a chemical probe for bromo and extra C-terminal bromodomain inhibition through optimization of a fragment-derived hit. *Journal of medicinal chemistry* **55**, 9831 (Nov 26, 2012).

16. S. Picaud *et al.*, PFI-1, a highly selective protein interaction inhibitor, targeting BET Bromodomains. *Cancer research* **73**, 3336 (Jun 1, 2013).

17. C. W. Chung, A. W. Dean, J. M. Woolven, P. Bamborough, Fragment-based discovery of bromodomain inhibitors part 1: inhibitor binding modes and implications for lead discovery. *Journal of medicinal chemistry* **55**, 576 (Jan 26, 2012).

18. M. Philpott *et al.*, Bromodomain-peptide displacement assays for interactome mapping and inhibitor discovery. *Molecular bioSystems* **7**, 2899 (Oct, 2011).

19. T. N. Pathiraja *et al.*, TRIM24 links glucose metabolism with transformation of human mammary epithelial cells. *Oncogene* **34**, 2836 (May 28, 2015).

20. W. W. Tsai *et al.*, TRIM24 links a non-canonical histone signature to breast cancer. *Nature* **468**, 927 (Dec 16, 2010).

21. E. Nicodeme *et al.*, Suppression of inflammation by a synthetic histone mimic. *Nature* **468**, 1119 (Dec 23, 2010).

22. M. Ceribelli *et al.*, Blockade of oncogenic IkappaB kinase activity in diffuse large B-cell lymphoma by bromodomain and extraterminal domain protein inhibitors. *Proceedings of the National Academy of Sciences of the United States of America* **111**, 11365 (Aug 05, 2014).

23. S. Miyoshi, K. Iwata, H. Hikawa, K. Sugaraha. Antitumor Agent. International Patent No PCT/JP2008/073864 (WO/2009/084693)2009 PCT/JP2008/073864, 2009;

24. P. Filippakopoulos *et al.*, Benzodiazepines and benzotriazepines as protein interaction inhibitors targeting bromodomains of the BET family. *Bioorganic & medicinal chemistry* **20**, 1878 (Mar 15, 2012).

25. J. C. Borah *et al.*, A small molecule binding to the coactivator CREB-binding protein blocks apoptosis in cardiomyocytes. *Chemistry & biology* **18**, 531 (Apr 22, 2011).

26. S. Picaud *et al.*, RVX-208, an inhibitor of BET transcriptional regulators with selectivity for the second bromodomain. *Proceedings of the National Academy of Sciences of the United States of America*, (Nov 18, 2013).

27. L. Wang, J. Pratt, K. McDaniel. (WO2013097052) BROMODOMAIN INHIBITORS (W. I. P. Organization, PCT/CN2011/002224, 2013; https://patentscope.wipo.int/search/en/detail.jsf?docId=WO2013097052)

28. L. A. Hasvold, D. Liu, P. C. H., P. J. K., G. S. Sheppard. (WO2013155695) ISOINDOLONE DERIVATIVES (W. I. P. Organization, PCT/CN2012/074411, 2013; https://patentscope.wipo.int/search/en/detail.jsf?docId=WO2013155695)

29. R. D. Hubbard *et al.* (WO2013185284) PYRIDINONE AND PYRIDAZINONE DERIVATIVES (W. I. P. Organization, PCT/CN2012/076748, 2013; http://patentscope.wipo.int/search/en/WO2013185284)

30. Sachchidanand *et al.*, Target structure-based discovery of small molecules that block human p53 and CREB binding protein association. *Chemistry & biology* **13**, 81 (Jan, 2006).

31. L. Anders *et al.*, Genome-wide localization of small molecules. *Nature biotechnology* **32**, 92 (Jan, 2014).

32. P. Ciceri *et al.*, Dual kinase-bromodomain inhibitors for rationally designed polypharmacology. *Nature chemical biology* **10**, 305 (Apr, 2014).

33. S. W. Ember *et al.*, Acetyl-lysine binding site of bromodomain-containing protein 4 (BRD4) interacts with diverse kinase inhibitors. *ACS chemical biology* **9**, 1160 (May 16, 2014).

34. A. Dittmann *et al.*, The commonly used PI3-kinase probe LY294002 is an inhibitor of BET bromodomains. *ACS chemical biology* **9**, 495 (Feb 21, 2014).

35. Library of Integrated Network-based Cellular Signatures. "HMS LINCS Database" (Harvard Medical School; NIH LINCS Program, http://lincs.hms.harvard.edu/db/)

36. X. Deng *et al.*, Characterization of a selective inhibitor of the Parkinson's disease kinase LRRK2. *Nature chemical biology* **7**, 203 (Apr, 2011).

37. B. D. Lee, V. L. Dawson, T. M. Dawson, Leucine-rich repeat kinase 2 (LRRK2) as a potential therapeutic target in Parkinson's disease. *Trends in pharmacological sciences* **33**, 365 (Jul, 2012).

38. J. Schulze *et al.*, Cell-based protein stabilization assays for the detection of interactions between small-molecule inhibitors and BRD4. *Journal of biomolecular screening* **20**, 180 (Feb, 2015).

39. J. Zuber *et al.*, RNAi screen identifies Brd4 as a therapeutic target in acute myeloid leukaemia. *Nature* **478**, 524 (Oct 27, 2011).

Chapter 4

Concluding Remarks: Application of Novel Assay Platforms toward the Discovery of CBP Bromodomain Inhibitors

Contributors: Katharin Shaw, Dennis Buckley, Michael McKeown, Jinhua Wang, Nick Kwiatkowski, Nathanael Gray, James Bradner

Discovery of a CBP Bromodomain Inhibitor

Kinase inhibitors have been recently discovered to inhibit bromodomains with up to nanomolar potencies (*1-3*). Among bromodomains, these molecules have demonstrated a high degree of selectivity for the BET family. However, through our studies in collaboration with DiscoveRx, we discovered kinase inhibitors that also demonstrate some activity against non-BET bromodomains, including CBP and P300 (Figure 3.9, 3.10). Since we have previously found that modification off of a core scaffold has the potential to define bromodomain selectivity, we decided to mine kinase inhibitors for a lead on a CBP/P300-selective compound. Toward this goal, the assay platform designed around CBP in Chapter 2 and the novel bromodomain profiling platform in Chapter 3 work in concert to enable the discovery of small molecule inhibitors of the CBP/P300 bromodomain.

Kinase library screening

We collaborated with the Gray laboratory to screen a library of approximately 400 kinase inhibitors, diverse in scaffold and biological target. Compounds were tested in 4-point dose in AlphaScreen assays of both BRD4(1) and CBP in order to gain an approximate understanding of their selectivity. Of the compounds screened, the majority of compounds with dual kinase-bromodomain activity inhibited BRD4, and most of the small molecules that did inhibit CBP demonstrated inhibited BRD4 more strongly. However, several compounds in the same structural class as XMD11-50 (particularly, XMD12-70-2 and XMD12-3-2) showed a marked preference for CBP over BRD4 (Figure 4.1).

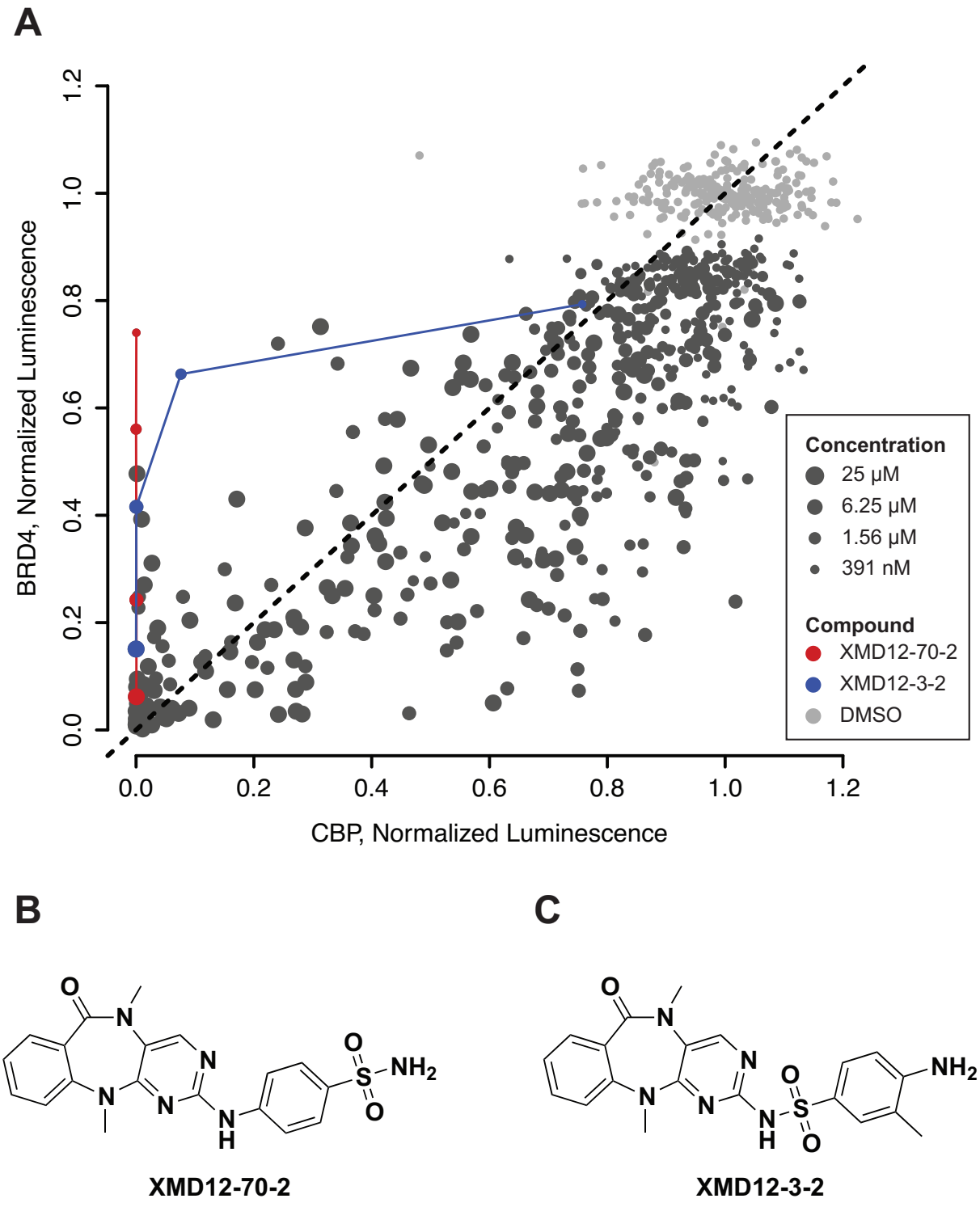

Figure 4.1 Kinase Inhibitor Library Screening (A) Subset of the kinase inhibitor library tested at four doses against BRD4(1) bromodomain and CBP bromodomain in AlphaScreen assay **(B)** Chemical structure of XMD12-70-2 **(C)** Chemical structure of XMD12-3-2

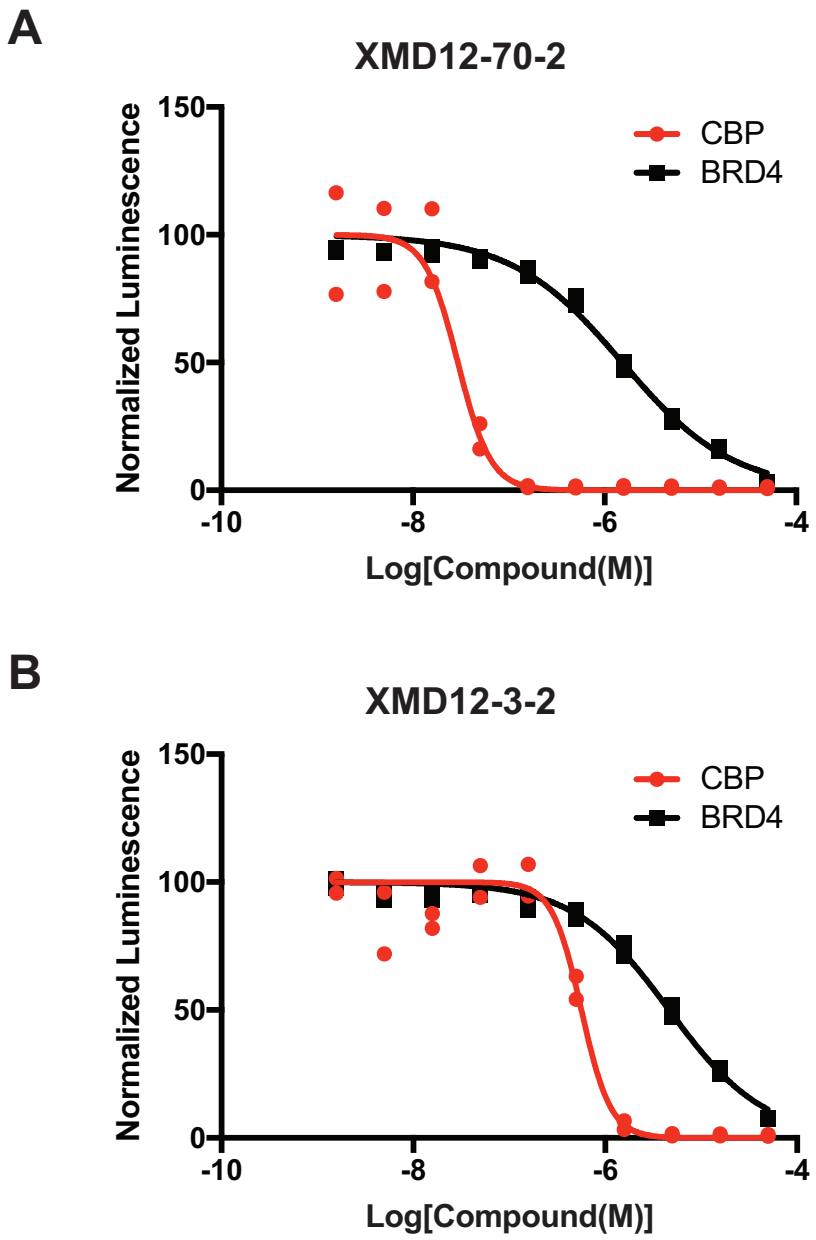

Figure 4.2 AlphaScreen Assay of Cherry Picks (A) AlphaScreen assay of XMD12-70-2 against CBP and BRD4 **(B)** AlphaScreen assay of XMD12-3-2 against CBP and BRD4

Selectivity profiling

We then cherry picked these compounds and evaluated them further in both CBP and BRD4 AlphaScreen assays. Testing these compounds in 10-point dose response confirmed their selectivity for CBP over BRD4 (Figure 4.2). XMD12-70-2 was approximately 50-fold more selective for CBP (IC50 = 29.4 nM) over BRD4 (IC50 = 1.53 μM), and XMD12-3-2 was approximately 8-fold more selective for CBP (IC50 = 565 nM) over BRD4 (IC50 = 4.64 μM). Based on these data, we chose XMD12-70-2 for further evaluation. The compound was resynthesized by Dennis Buckley and sent to BROMO*scan* to verify binding constants. The resynthesized compound demonstrated potent CBP binding (K_D = 23 nM) and was approximately 8-fold more selective for CBP than for BRD4(1) (K_D = 180 nM) (Figure 4.3).

Cellular activity of XMD12-70-2

The compound was subsequently testing in the CBP bromodomain BRET assay in order to determine the ability of the small molecule to engage the CBP bromodomain in a cellular context. Cells were treated with 10 μM and 500 nM of XMD12-70-2. The literature reported CBP bromodomain inhibitor SGC-CBP30 (*4*) was used as a positive control in the assay. At 10 μM, XMD12-70-2 exhibited 26% inhibition. There was no significant difference in signal between 500 nM XMD12-70-2 and the DMSO control (Figure 4.4).

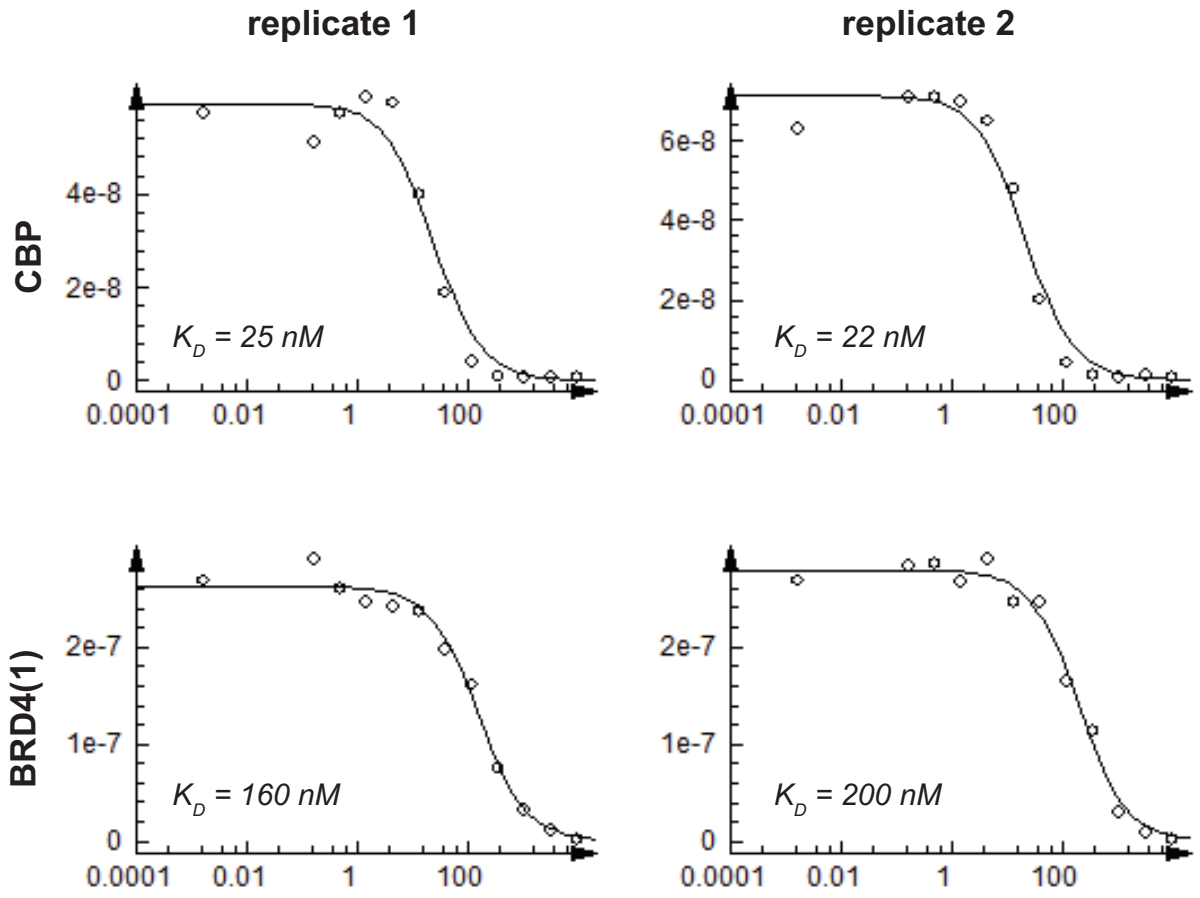

Figure 4.3 Binding Constant Determination by BROMO*scan* Amount of bromodomain measured by qPCR is plotted against compound concentration in nM

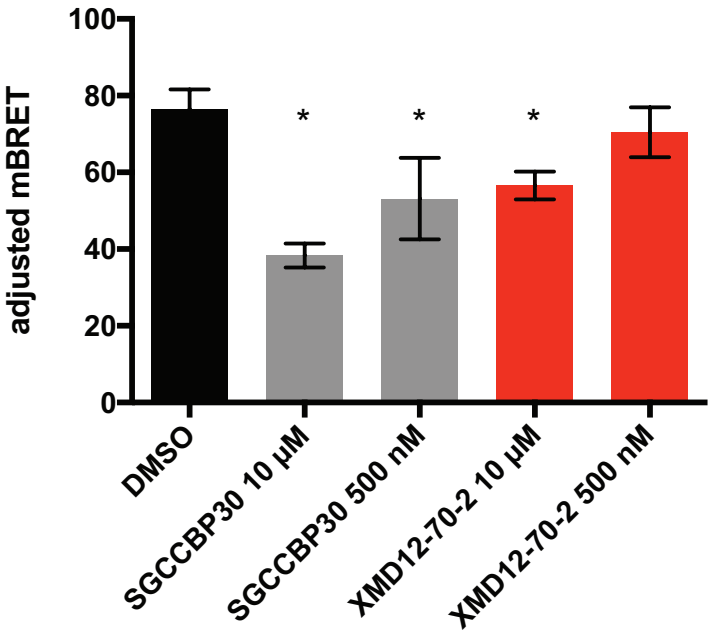

Figure 4.4 CBP Bromodomain BRET Assay Cells were treated with 10 µM and 500 nM of XMD12-70-2. The literature reported compound SGC-CBP30 was used as a positive control. Asterisk denotes a p-value of <0.01 in a t-test compared to the vehicle control.

Further research

Medicinal chemistry should be performed around the scaffold to determine structure-activity relationships and improve on CBP selectivity, if possible. Moreover, the compound should be modified in such a way as to remove kinase inhibition. While it is likely that the BET subfamily is the primary concern for compound promiscuity among bromodomains, a full BROMO*scan* panel needs to be performed to in order to determine CBP selectivity. The BRET studies should be expanded to include CBP bromodomain/histone acetyltransferase and full-length proteins in order to determine whether or not inhibition of the CBP bromodomain precludes chromatin binding.

Conclusion

In this dissertation, two different types of assay platforms were developed and implemented. In Chapter 2, I discussed a chemical biology assay platform for the development of CBP bromodomain inhibitors, and it encompassed both biochemical and cellular assays. The platform was designed to assess small molecule inhibition of the CBP bromodomain in a robust, high-throughput manner, allowing for both screening and iterative medicinal chemistry. Promising compounds were more deeply scrutinized, ensuring target engagement within a cellular context. In Chapter 3, I discussed the development and validation of the BROMOscan assay platform and then its use in the discovery of non-BET family bromodomain inhibitors. As opposed to testing a large number of small molecules against a single bromodomain, BROMOscan enables the profiling of small molecules against bromodomains across each subfamily, yielding information about compound specificity.

Used in conjunction with one another, these two assay platforms are powerful tools in the development of potent, selective, and cellularly active small molecule inhibitors of CBP. The data discussed in this chapter establish that this is an effective strategy for the development of non-BET bromodomain inhibitors. The flexibility of the assays used enable this strategy to be adapted for other bromodomain targets in the future, providing a means to develop chemical probes for inhibitors across the bromodomain family.

References

1. S. W. Ember *et al.*, Acetyl-lysine binding site of bromodomain-containing protein 4 (BRD4) interacts with diverse kinase inhibitors. *ACS chemical biology* **9**, 1160 (May 16, 2014).
2. M. P. Martin, S. H. Olesen, G. I. Georg, E. Schonbrunn, Cyclin-dependent kinase inhibitor dinaciclib interacts with the acetyl-lysine recognition site of bromodomains. *ACS chemical biology* **8**, 2360 (Nov 15, 2013).
3. P. Ciceri *et al.*, Dual kinase-bromodomain inhibitors for rationally designed polypharmacology. *Nature chemical biology* **10**, 305 (Apr, 2014).
4. A. Hammitzsch *et al.*, CBP30, a selective CBP/p300 bromodomain inhibitor, suppresses human Th17 responses. *Proc Natl Acad Sci U S A* **112**, 10768 (Aug 25, 2015).

Appendix A

Supplementary Materials for Chapter 3

Contributors: Katharin Shaw, Jun Qi, Michael McKeown, Xiang Xu, Alexander Federtion, William B. Smith, Roodolph St. Pierre Dennis Buckley, Minoru Tanaka, Stuart W. Ember, Ernst Schonbrunn, Matt Lindon, Jeremy P. Hunt, Lisa M Wodicka, Gabriel Pallares, Pietro Ciceri, Mark Floyd, Adam D. Torrey, Daniel K. Treiber, James Bradner

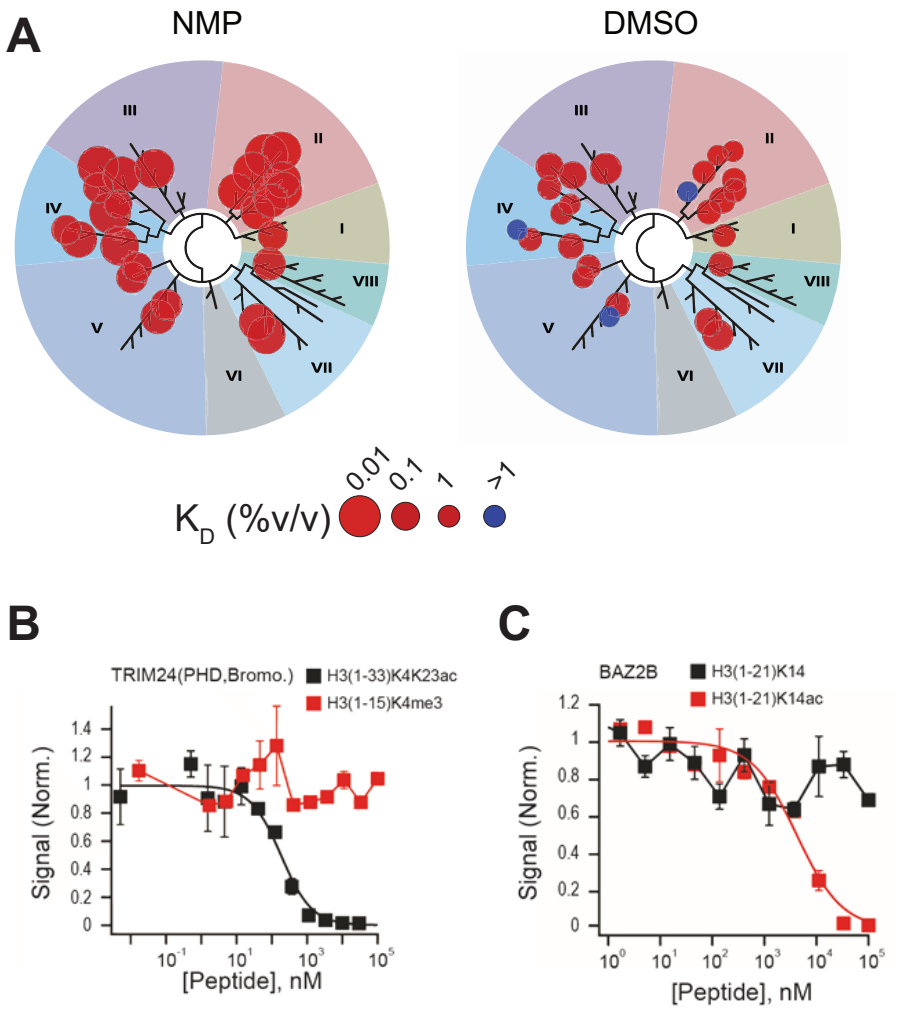

Figure S3.1 BROMO*scan* Assay Validation Using Solvents and Acetylated Peptides (A) Interaction maps demonstrating NMP and DMSO binding to bromodomains **(B)** TRIM24 binds to reported acetylated peptide but not to the corresponding non-acetylated peptide **(C)** BAZ2Bbinds to reported acetylated peptide but not to the corresponding non-acetylated peptide

A

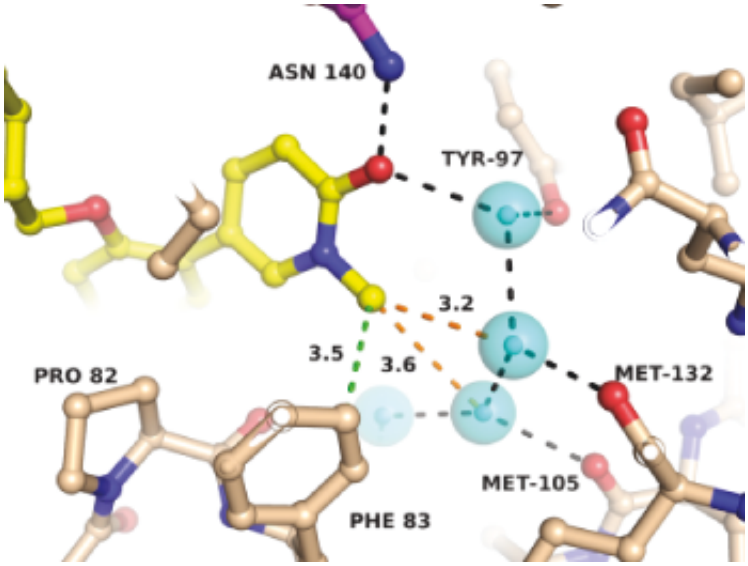

B

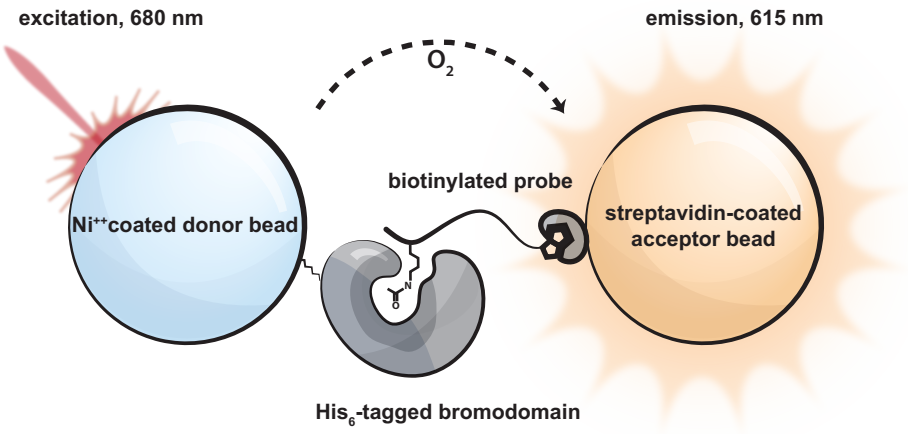

C

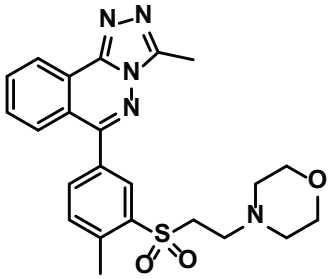

20

Figure S3.2 Discovery of Novel Bromodomain Inhibitors (A) Co-crystal of MT1 and BRD4(1) **(B)** Schematic of AlphaScreen assay **(C)** Chemical structure of compound 20, a screening hit in the CBP AlphaScreen assay

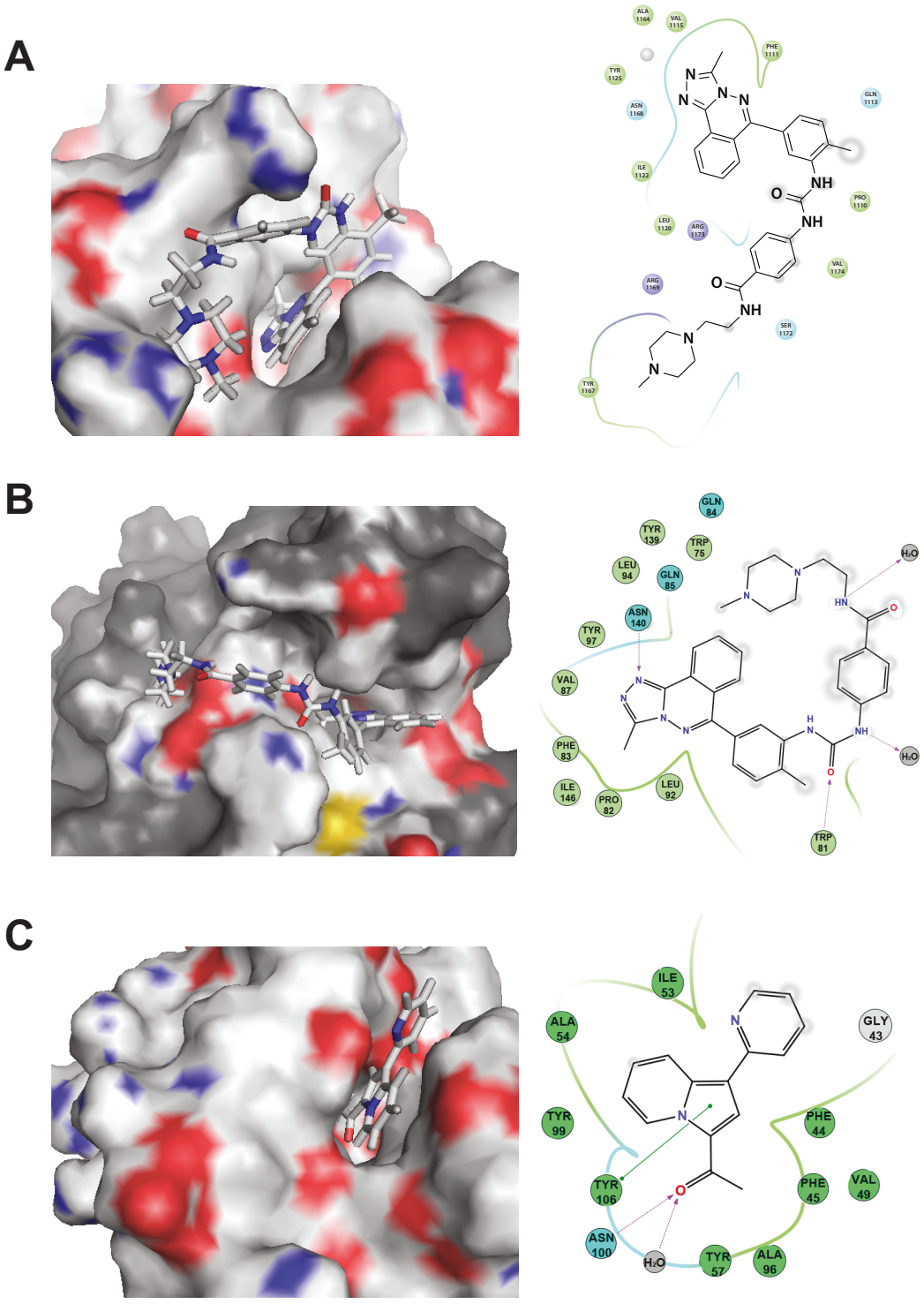

Figure S3.3 Computation Docking into Crystal Structures (A) Docking of KS2222 into CBP bromodomain **(B)** Docking of KS2222 into BRD4(1) bromodomain **(C)** Docking of GW334556X into BRD9 bromodomain

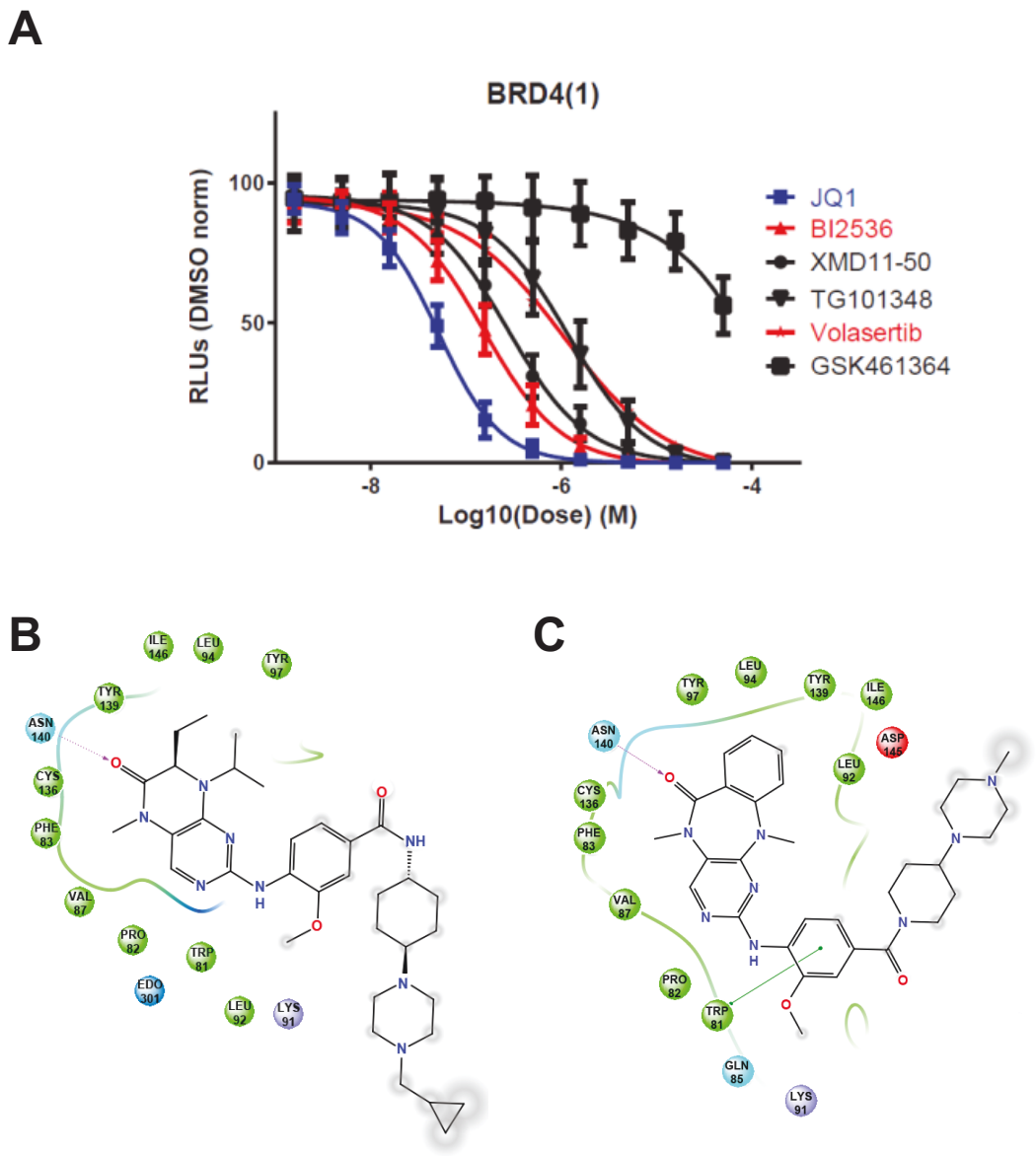

Figure S3.4 Characterization of Dual Kinase-Bromodomain Inhibitors (A) Kinase inhibitors tested in BRD4(1) AlphaScreen assay **(B)** Ligand interaction diagram of BI-6727/volasertib and BRD4(1) in co-crystal structure **(C)** Ligand interaction diagram of XMD11-50 and BRD4(1) in co-crystal structure

A

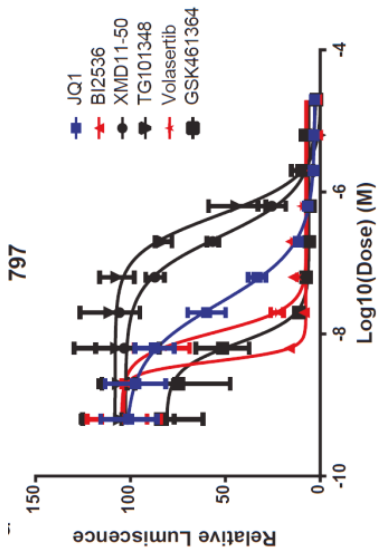

Compound Name	EC50 (μM)	Hill	Curve Bottom	Curve Top	Max Response
(+)-JQ1	0.65177	1.03	1	105.5	100
BI-2536	1.2259	1.15	1.3	80	72.348
BI-5727	0.99459	1.05	0.1	50	42.075
GSK-461364A	>10				3.7275
(+)-JQ1	1.1872	0.99	-1	100	93.1
NVP-TAE-684	>10				2.468
XMD11-50	3.392	1.09	1.9	121.7	92.369

B

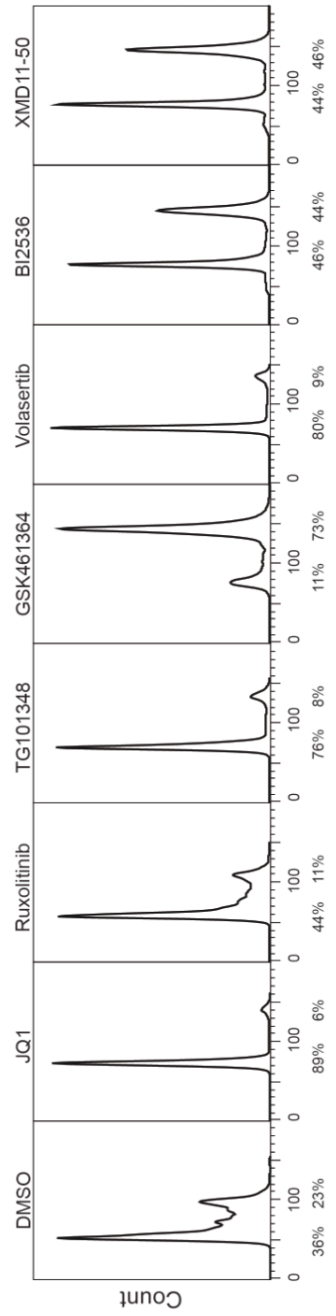

Figure S3.5 Cellular Activity of Dual Kinase-Bromodomain Inhibitors (A) Cellular viability of 797 cells treated with kinase inhibitor set **(B)** Cell cycle studies of kinase inhibitor set in BRD4-dependent 797 cells

Supplementary Table 1. Bromodomains studied in this report

Bromodomain	Entrez Gene Symbol	Accession Number	Amino Acid Start/Stop	Included in Initial 10 μM Screen
BAZ2B	BAZ2B	NP_038478.1	S1858/S1972	Yes
BRD1	BRD1	NP_055392.1	E556/A688	Yes
BRD2(1)	BRD2	NP_005095.1	K71/N194	Yes
BRD2(2)	BRD2	NP_005095.1	E348/D455	Yes
BRD3(1)	BRD3	NP_031397.1	P24/E144	Yes
BRD3(2)	BRD3	NP_031397.1	G306/P416	Yes
BRD4(1)	BRD4	NP_490597.1	N44/E168	Yes
BRD4(2)	BRD4	NP_490597.1	K333/E460	Yes
BRDT(1)	BRDT	NP_001717.2	N21/E137	Yes
BRDT(2)	BRDT	NP_001717.2	K250/E382	Yes
CBP	CREBBP	NP_004371.1	R1081/G1197	Yes
TAF1(2)	TAF1	NP_004597.2	D1521/D1656	Yes
ATAD2A	ATAD2	NP_054828.2	Q981/R1108	No
ATAD2B	ATAD2B	NP_060022.1	Q955/R1082	No
BAZ2A	BAZ2A	NP_038477.2	M1792/L1905	No
BRD9	BRD9	NP_076413.2	L14/Q143	No
BRPF1	BRPF1	NP_004625.2	E627/G740	No
BRPF3	BRPF3	NP_056510.2	E588/G701	No
EP300	EP300	NP_001420.2	A1040/G1161	No
FALZ	BPTF	NP_872579.2	S2791/H2911	No
PBRM1(2)	PBRM1	NP_060635.2	S178/E291	No
TAF1L(2)	TAF1L	NP_722516.1	Q1523/D1654	No
TRIM24(PHD,Bromo.)	TRIM24	NP_003843.3	P790/P977	No
TRIM33(PHD,Bromo.)	TRIM33	NP_056990.3	D882/A1087	No
WDR9(2)	BRWD1	NP_061836.2	A1310/E1430	No

Supplementary Table 2. Capture ligands used for BROMO*scan* assays

Bromodomain	Bait Molecule	Bait Molecule Type
BRD2(1)	I-BET	Small Molecule
BRD2(2)		
BRD3(1)		
BRD3(2)		
BRD4(1)		
BRD4(2)		
BRDT(1)		
BRDT(2)		
BRD9	GW334556X	
PBRM1(2)	H3(11-31)K14acK18acK23acK27ac	Modified Histone Peptide
BAZ2B	H3(1-21)K4K9K14acK18	
TRIM33(PHD,Bromo.)	H3(1-23)K4K9me3K14K18acK23	
TRIM24(PHD,Bromo.)	H3(1-33)K4K9K14K18K23acK27	
CREBBP	H3(47-65)K56acK64	
EP300		
ATAD2A	H4(1-20)K5acK8acK12acK16ac	
ATAD2B		
BAZ2A		
BRD1		
BRPF1		
BRPF3		
FALZ		
TAF1(2)		
TAF1L(2)		
WDR9(2)		